August 2011

Ph.D. Dissertation

The Role of MMR on the Non-Homologous End Joining Activity

Graduate School of Chosun University

Department of Bio-Materials

Ankita Shahi (De)

The Role of MMR on the Non-Homologous End Joining Activity

이중나선 절단에 따른 DNA손상복구 과정에서 MMR의 역할연구

25th August 2011

Graduate School of Chosun University

Department of Bio-Materials

Ankita Shahi (De)

The Role of MMR on the Non-Homologous End Joining Activity

Advisor: Prof. Ho-Jin You

A dissertation submitted to the Graduate School of Chosun University in partial fulfillment of the requirements for the degree of Doctor of Philosophy in Science

April 2011

Graduate School of Chosun University

Department of Bio-Materials

Ankita Shahi (De)

The Ph.D. dissertation of Ankita Shahi (De) is certified by

Chairman	**Chosun Univ.**	**Prof.**	**In-Youb Chang**	**_____**
Committee Members:				
	Chosun Univ.	**Prof.**	**Jae-Yeoul Jun**	**_____**
	Chosun Univ.	**Prof.**	**Young-Jin Jeon**	**_____**
	Chosun Univ.	**Prof.**	**Ho Jin You**	**_____**
	Chosun Univ.	**Prof.**	**Jung-Hee Lee**	**_____**

June 2011

Graduate School of Chosun University

CONTENTS

LIST OF FIGURES

LIST OF ABBREVIATIONS

MMR	mismatch repair
DSB	double strand break
NCS	neocarzinostatin
IR	irradiation
NHEJ	non-homologous end joining
HR	homologous recombination
DNA-PKcs	DNA dependent protein kinase catalytic subunit
XRCC4	X-ray repair complementing defective repair in Chinese hamster cells 4
WRN	Werner syndrome
V(D)J	variable diverse and joining
HNCCP	Hereditary nonpolyposis colorectal cancer
ICLs	inter-strand cross-links
TCR	Transcription-coupled repair
shRNA	short hairpin RNA
cDNA	complementary DNA
HA	hemagglutinin
DNA-BD	DNA binding domain
EDTA	Ethylenediaminetetraacetic acid
PVDF	Polyvinylidene Fluoride
PBS	phosphate buffer saline
DAPI	4',6-diamidino-2-phenylindole

NaOH	sodium hydroxide
GFP	green fluorescent protein
PCNA	Proliferating Cell Nuclear Antigen
NTR	N terminal region
RT-PCR	Reverse transcription polymerase chain reaction

<국문 초록>

이중나선 절단에 따른 DNA손상복구 과정에서 MMR의 역할연구

Ankita Shahi (De)
지도교수: 유호진
조선대학교 대학원 생물신소재 학과

MSH6는 mismatched DNA base를 복구하는데 중요한 역할을 하는 단백질로 널리 알려져 있다. 그러나 최근연구들은 여러 DNA손상복구 pathway는 연관되어 있다고 보고되고 있음으로 mismatched DNA 손상복구에 관여하는 MSH6 또한 다른 DNA손상복구에도 관여 할 수 있음을 시사한다. 본 연구에서는 결합 단백질을 조사하는 yeast two-hybrid를 통해 MSH6는 Ku70과 결합함을 보았다. Ku70은 DNA-dependent protein kinase의 중요한 조절자로서 Ku86과 복합체를 이루며, DNA의 이중나선절단에 따른 손상복구에 중요한 역할을 하는 단백질이다. mismatched DNA손상복구에 중요한 MSH6가 DNA이중나선절단 복구에 관여하는 Ku70과 결합은 다양한 DNA 손상복구 과정들이 상호 연관됨을 암시한다. 먼저 세포 수준에서 MSH6와 Ku70의 결합을 확인하였고, 이두 단백질의 결합은 방사선 조사(ionizing radiation, IR)나 neocarzinostatin(NCS)에 의해 증가함을 확인하였다. 또한 과발현실험을 통해 이 두 단백질의 결합이 직접적인 결합임을 증명하였다. MSH6는 정상세포에서는 핵내에 산발적으로

존재하나, IR이나 NCS같은 DNA 이중나선절단 유도시엔 DNA foci를 이룸을 면역염색법을 통해 관찰하였다. 이런 MSH6 foci는 DNA 손상반응 유도시 Ku70과 공존(colocalization)하며, DNA손상 marker인 γ-H2AX와도 공존하면서 MSH6 foci가 DNA damage foci임을 증명하였다. 다음으로 두 단백질의 결합에 따른 DNA손상복구에 미치는 영향을 조사하기 위해, MHS6가 결핍된 세포주를 제작하였다. MSH6 결핍 세포주에서 이중나선절단에 따른 복구가 정상세포에 비해 감소함을 comet assay를 통해 확인하였다. 또한 MSH6 과발현에 의해 DNA손상복구의 감소가 회복됨을 보았다. 또한 clonal survival assay를 통해 MSH6가 결핍된 세포는 정상세포에 비해 IR에 민감함을 확인하였고 γ-H2AX foci또한 감소하였다. 따라서, 본 연구 결과는 mismatched DNA 복구에 관여하는 MSH6가 Ku70과의 결합을 통해 이중나선 절단에 따른 비상동말단결합 과정에 관여함을 증명하였다. 이는 MMR단백질이 mismatched DNA 복구외에 이중나선절단에 따른 복구에도 관여함을 증명함으로써 여러 다양한 DNA손상복구 과정들은 상호 연관되어 있음을 시사한다.

I. Introduction

Double- stranded DNA break (DSBs) and DNA damage signaling are included as important parts of a large pool of biological processes that are crucial to maintaining genomic stability. Double- stranded DNA break (DSBs) can be introduced by any agents includes endogenous factors like metabolic products and reactive oxygen species, and also exogenous factors like ionizing radiation and certain drugs (Khanna and Jackson, 2001). The failure to repair DSBs, or mis-repair, can result in cell death or large-scale chromosome changes including deletions, translocations, and chromosome fusions that enhance genome instability and are hallmarks of cancer cells. Cells have evolved groups of proteins that function in signaling networks that sense DSBs or other DNA damage, arrest the cell cycle, and activate DNA repair pathways (Shrivastav et al., 2008). Two distinctly different pathways that mediate DSB repair have been identified in mammalian cells: homologous recombination (HR) and non- homologous end joining (NHEJ) (Weterings and Chen, 2008).

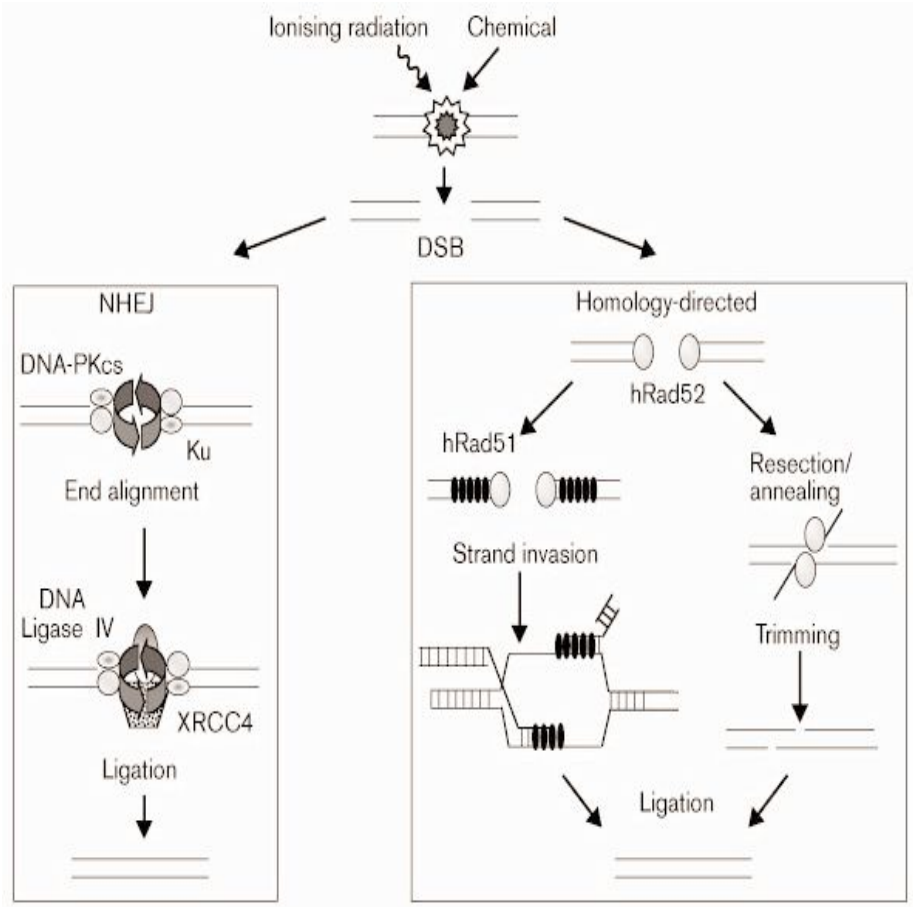

Figure 1 Pathways of DSB repair. The scheme is based on (Karran, 2000).

The two pathways differ in their fidelity and template requirements (Mao et al., 2008). HR utilizes the homologous sister chromatid or homologous chromosome as a template, resulting in error-free repair of the missing information in the damaged DNA. In contrast, NHEJ is referred as an intrinsically error- prone pathway because this process joins the two broken-DNA ends without using a homologous template. In NHEJ, the bases are usually deleted or inserted prior to healing of the DSB. NHEJ requires no template and is sometimes facilitated by the

annealing of short homologous sequences. Despite the mutagenic nature of NHEJ, this pathway is considered to be an important means for DSB repair in higher eukaryotes (Bannister et al., 2004).

Thus, the choice of DSB repair pathway determines the fidelity of repair, which in turn may influence the rates of aging and tumorigenesis. Both DSB repair pathways play important roles in mammalian DSB repair. The exact mechanism by which the choice between the two DSB repair pathways is made remains unclear (Mao et al., 2008).

A. Role of Ku70 in mammalian cell and its interacting partners

In cells, NHEJ involves a DNA end-binding heterodimer of the Ku70 and Ku80 proteins which activates the catalytic subunit (DNA-PKcs) of DNA-dependent protein kinase (DNA-PK) by stabilizing its interaction with DNA ends. The Ku-DNA complex acts as a scaffold for the association of a 460-kDa serine/ threonine kinase:DNA- PKcs. This interaction between Ku and DNA-PKcs is thought to be mediated by the Ku80 carboxyl-terminus. This facilitates rejoining by a DNA ligase IV/Xrcc4 (X-ray cross complementing 4) heterodimer (Karran, 2000).

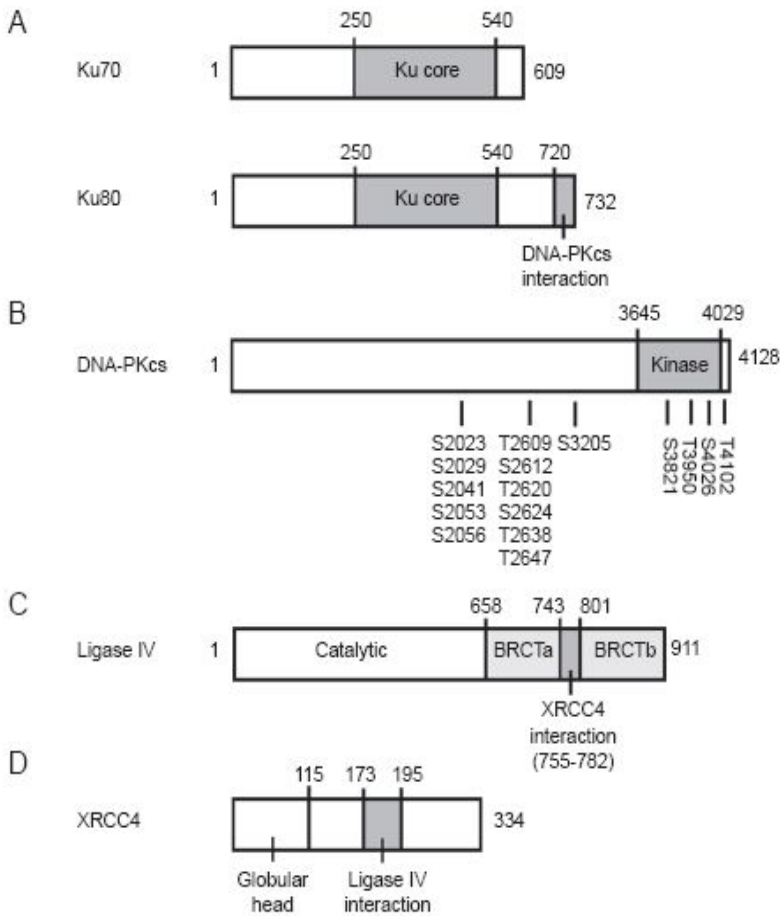

Figure 2 Schematic representations of the human NHEJ core enzymes. **(A)** The central regions of the Ku70 and the Ku80 protein (the 'Ku core' domains, roughly encompassing residues 250-540) mediate both the hetero-dimerization of Ku70 and Ku80 and the interaction of the Ku70/80 heterodimer with the DNA helix. The association of the Ku70/80 heterodimer with DNA-PKCS is thought to be mediated by the extreme carboxyl-terminus of Ku80. **(B)** The serine/threonine kinase domain of DNA-PKCS is located in the carboxy-terminus, between residues 3645 and 4029. All known phosphorylation sites are indicated: the 2056 cluster, the 2609 cluster,

and the carboxyl-terminal cluster. **(C)** The ligase IV protein possesses a BRCT tandem that encompasses residues 658-911, but the domain that mediates the interaction between ligase IV and XRCC4 is located in between the two BRCT regions, spanning residues 755-782. Several domains necessary for the catalytic activity of ligase IV are situated in the amino-terminal region. **(D)** The first 115 amino acids of the XRCC4 protein form a globular head, while the rest of the molecule forms a long stalk which interacts with ligase IV between residues 173 and 195 (Weterings and Chen, 2008).

The Ku proteins were originally identified as autoantigens in patients with scleroderma polymyositis syndrome (Mimori et al., 1986). Ku70 is made up of 609 amino acids, generating a 70-kDa protein, and forms a heterodimer with the 80-kDa Ku86 subunit (also known as Ku80), which consists of 732 amino acids. Both Ku proteins have an intrinsic nuclear localization signal and primarily localize to the nucleus (Koike et al., 2001). Ku70 and Ku86 show only 14% homology to one another. However, structural analysis of the two proteins bound to double-stranded DNA has shown that the two proteins are structurally similar, despite the lack of sequence homology.

Ku proteins are multifunctional proteins that possess deubiquitylation activity and play a key role in DNA repair and transcriptional regulation (Tuteja and Tuteja, 2000; Nolens et al., 2009; Yin and Glass, 2006; Amsel et al., 2008). Substantial biochemical evidence also indicates that various proteins physically interact with the Ku complex. For example, Ku70/80 interacts with both the protein and RNA components of human telomerase, suggesting that the Ku complex is involved in telomere maintenance in higher eukaryotes (Ting et al., 2005; Chai et al., 2002). The Ku complex has been shown to inhibit apoptosis through an association with the proapoptotic factor Bax (Cohen et al., 2004). Interactions between Ku70 and

p18-cyclin E, and Ku70 and Bax, provide a balance between apoptosis and cell survival in response to genotoxic stress (Mazumder et al., 2007). Ku70 interacts with Runx3 in the nucleus, suggesting a possible link between a tumor suppressor function and DNA repair (Tanaka et al., 2007). The human Werner-syndrome protein (WRN), which is a member of the RecQ helicase family, also interacts with Ku70/80, and these proteins are thought to serve a function in one or more pathways of DNA metabolism (Li and Comai, 2000; Karmakar et al., 2002). The Ku70/80 complex also binds RAG1, providing a biochemical link between the two phases of V(D)J recombination. Furthermore, the cell polarity protein Par3 plays a role in efficient repair of DSBs through association with the DNA–PK complex (Fang et al., 2007).

B. MMR mediates DNA damage signaling

In recent years considerable progress has been made toward identifying DSB repair proteins and elucidating repair mechanisms, although a thorough understanding of exactly how DSB repair is accomplished and how a cell "chooses" which repair pathway to use has not yet been realized (Bannister et al., 2004). It has become clear that a single protein can play multiple roles in DNA repair and damage response pathways and in other DNA transactions. In human multiple proteins are available which plays many important roles including DNA damage repair and maintaining genomic integrity. DNA mismatch repair (MMR) proteins are one such example. MMR is highly conserved repair system and defective MMR is strongly associated with HNCCP. MMR deficiency and epigenetic silencing of MMR gene expression leads to cancer development. In addition to its role in correcting mismatches formed during replication, MMR has

been implicated in the cellular DNA damage response (Iyer et al., 2006; Stojic et al., 2004).

MMR proteins not only promote DNA damage-induced cell cycle arrest and apoptosis but also play an important role in other metabolic pathways. Recent studies implicate MMR in repair of ICLs, in a process that involves protein components from homologous recombination, double strand break repair, and nucleotide excision repair (Li, 2008). MMR proteins are ubiquitous players in a diverse array of important cellular function. A number of interaction between MMR proteins and DNA damage signaling proteins have been reported including interactions between MSH2 and ATR, Chk1 and Chk2 (Wang and Qin, 2003); MLH1 and ATM; PMS2 and P73 ; the three MutL homologues, MLH1, PMS2, and PMS1 with a large number of proteins involved in cell cycle/ signaling/apoptosis function.

MMR proteins participate in a number of other cellular processes including recombination processes that have been most extensively studied in fungi. A second function of MMR in recombination is its ‘‘antirecombination’’ role in which recombination between related but distinct sequences (known as homologous recombination) is inhibited by the MMR system. A third function of MMR in recombination involves two MutS homologues, MSH2 and MSH3. MSH2–MSH3 acts in concert with Rad1–Rad10 endonuclease to trim nonhomologous DNA ends from a recombination pairing intermediate formed by annealing at a DSB between directly repeated sequences. MMR is involved in the generation of immunoglobulin diversity. Antibody diversity requires V(D)J recombination, class isotype switching, and somatic hypermutation in regions encoding the variable regions of immunoglobulin genes in B lymphocytes (Hsieh and Yamane, 2008).

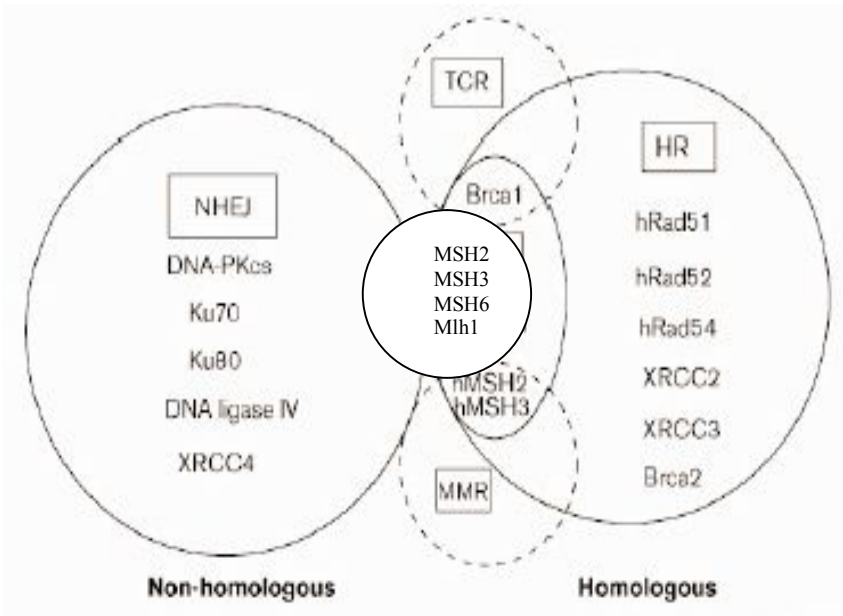

Figure 3 Proteins involved in DSB repair. The circle on the left contains a list of the MMR protein known to participate in NHEJ. Gene products involved in DSB repair by homology directed recombination (HR) are indicated in the large circle to the right. The SSA pathway which requires some degree of homology between joined termini is depicted as a sub-pathway of HR. Possible overlaps with the human excision (TCR) and MMR pathways are indicated. The scheme is based on (Karran, 2000).

In addition to repairing base–base mispairs, as well as small insertion or deletion loops arising during DNA replication, some MMR components, including hMSH2, hMSH6 and hMLH1, participate in recombination, DSB repair, apoptosis and cell cycle regulation. Moreover, it has been suggested that MMR can play a role in double strand break repair, although the underlying mechanism remain unknown (Evans et al., 2000; Sugawara et al., 1997). It has been shown that MSH2

has a role in error-prone NHEJ repair in mammalian chromosome (Smith et al., 2005). In human cells, 85% of the MSH2 is found in the MSH2.MSH6 (Mutsα) complex compare to the partitions between MSH6 and MSH3.

In this study, Ku70 was associated physically with the mismatch repair (MMR) protein MSH6. MMR is a highly conserved DNA-repair pathway, and defective MMR is strongly associated with hereditary non-polyposis colorectal cancer (HNPCC) (Harfe and Jinks-Robertson, 2000). In addition to a role in correcting mismatches formed during replication, MMR has recently been implicated in DSB repair after exposure to γ-irradiation (Elliott and Jasin, 2001).

In this report, the results indicated that MSH6-deficient cells had a major DSB repair defect, shown by both the presence of γ-H2AX foci and by comet-tail analysis. Further biochemical analyses show that MSH6 knockdown or over-expression leads to down-regulation or up-regulation of NHEJ, respectively. These results suggest that MSH6 is involved in the repair of DSBs through a direct physical interaction with Ku70. In addition, the developing view of the NHEJ mechanism is presented here which is complex and regulated by not only the well known NHEJ pathways, but also a systematically coordinated cellular network.

II. Materials and Methods

A. Cell culture and drug treatment

The human cervix adenocarcinoma cell line HeLa and the human embryonic kidney cell line HEK293T were cultured in Dulbecco's modified Eagle's medium (Gibco-BRL, Grand Island, NY, USA). The DLD1 colon cancer cell line was cultured in RPMI-1640 medium (Gibco-BRL). In both cases, the media was supplemented with 10% heat-inactivated fetal bovine serum (Cambrex Corp., East Rutherford, NJ, USA), 100 units/ml penicillin, and 100 mg/ml streptomycin sulfate (Invitrogen, Carlsbad, CA, USA). All cells were maintained in a humidified incubator containing 5% CO_2 at 37^{o}C. HeLa and DLD1 cell lines were obtained from the American Type Culture Collection (ATCC, Rockville, MD, USA), and the HEK293T cell line was obtained from the Cornell Institute for Medical Research (New York, NY, USA). To induce DNA breaks, exponentially growing cells were treated with the radiomimetic drug neocarzinostatin (NCS; Sigma, St Louis, MO, USA) at a final concentration of 100ng/ml in fresh cell media or irradiated at 5 Gray (Gy) from ^{137}Cs source (Gammacell 3000 Elan irradiator, Best Theratronics, Ottawa, Canada) and allowed to recover at 37^{o}C for various amounts of time.

B. Generation of stable MSH6 knockdown clones

The pSilencer2.1–U6 neo vector was obtained from Ambion (Austin, TX, USA). Vectors for expression of hairpin siRNAs were constructed by inserting corresponding pairs of annealed DNA oligonucleotides into the pSilencer 2.1–U6 vector between the BamHI and HindIII restriction sites according to the manufacturer's instructions. The MSH6-specific target sequence was selected based

on an online shRNA application from Invitrogen (http://www.ambion.com/techlib/nisc/psilencer-converter.html) using the human MSH6 sequence as the reference sequence (GenBank Accession No. NM_000179.2). The target sequences were 5'-GCCAGACACUAAGGAGGA AdTdT-3' (sense) and 5'-UUCCUCCUUAGUGUCUGGC dTdT-3' (antisense) for MSH6 siRNA #1 and 5'-GCGACUGUUCUAUAACUUU dTdT-3' (sense) and 5'-AAAGUUAUAGAACAGUCGCdTdT-3' (antisense) for MSH6 siRNA #2. A non-targeting sequence, 5'-CCUACGCCACCAAUUUCGU dTdT-3' and 5'-ACGAAAUUGGUGGCGUAGG dTdT-3', was used as a negative control. To generate single knockdown clones, HeLa cells were transfected with pSilencer2.1–U6, pSilencer2.1–U6 MSH6 siRNA #1 or pSilencer2.1–U6 MSH6 siRNA #2. Twenty-four hours after transfection, 400 mg/ml G418 was added to the culture medium for selection. After selection, stable clones were analyzed by real-time RT-PCR and western blotting to confirm down regulation of MSH6.

C. Plasmid constructs

The full-length Ku70 cDNA was amplified from GM00637 human fibroblast cells by RT-PCR using the Ku70 primers 5'-AATCTCGAGATGTCAGGGTGGGAG-3' (sense) and 5'-AATGGGCCCTCAGTCCTGGAAGTG-3' (antisense). The amplified Ku70 cDNA construct was cloned into the mammalian expression vector pcDNA3 in-frame with the hemagglutinin (HA) tag. The Ku70 sequence was confirmed by automated DNA sequencing. The human MSH6 expression vector and its control vector were obtained from Origene (OriGene Technologies, Inc., Rockville, MD, USA).

D. Antibodies

The following antibodies were used for immunoblotting: mouse monoclonal anti-MSH6 (1:2000 BD Transduction Laboratories, Franklin Lakes, NJ, USA), mouse monoclonal anti-MSH2 (1:2000; Calbiochem, San Diego, CA, USA), monoclonal anti-Ku70 (1:2000; BD Transduction Laboratories), monoclonal anti-XRCC4 (BD Transduction Laboratories), monoclonal anti-$DNAPK_{CS}$ (1:2000; Santa Cruz Biotechnology, Santa Cruz, CA, USA), polyclonal anti-Ku86 (1:2000; Santa Cruz Biotechnology), monoclonal anti-HA tag (1:2000; Santa Cruz Biotechnology) and monoclonal anti-α-tubulin (1:8000; Neomarkers, Fremont, CA, USA). MSH6 foci were detected by immunofluorescence staining using the MSH6 antibody (H-141; Santa Cruz Biotechnology) at a 1:50 dilution. γ- H2AX foci were detected by immunofluorescence staining using the γ-H2AX mouse monoclonal antibody (JBW301), Upstate Biotechnology, Temecula, CA, USA) at a 1:200 dilution. Immunoprecipitations of endogenous and exogenous proteins were performed using rabbit polyclonal antibodies directed against MSH6 (ab50604; Abcam, Cambridge, UK) and Ku70 (H-308; Santa Cruz Biotechnology).

E. Yeast two-hybrid analysis

The full-length Ku70 was sub-cloned into pGBT9 vector, which expresses proteins fused to the GAL4-DNAbinding domain (DNA-BD) (Clontech, Mountain View, CA, USA). This vector was used as bait to screen a human prostate cDNA library fused to the GAL4 activation domain according to the manufacturer's (Clontech) instructions. Positive clones were verified by ono-on-one transformation and selection on agar plates lacking leucine and tryptophan (-LH) or adenine,

histidine, leucine and tryptophan (-AHLT) and also processes for a β-galactosidase assay.

F. Immunoprecipitation assay and western-blot analysis

Cells were lysed in ice-cold NP-40 lysis buffer [50mM Tris–HCl (pH 8.0), 150mM NaCl, 1% Nonidet P-40] containing ethylenediaminetetraacetic acid (EDTA)-free protease inhibitor cocktail (Roche, Basel, Switzerland). Equal amounts of proteins were then resolved on 6–15% SDS-PAGE gels, followed by electrotransfer to polyvinylidene difluoride membranes (Millipore, Bedford, MA, USA). The membranes were blocked for 2 h in TBS-t [10mM Tris–HCl (pH 7.4), 150mM NaCl, 0.1% Tween 20] containing 5% fat-free milk at room temperature and then incubated with the indicated primary antibodies overnight at 4^{o}C After incubation for 2 h with appropriate peroxidase conjugated secondary antibodies, developed using enhanced chemiluminescence detection system.

For the immunoprecipitation assay, aliquots of soluble cell lysates were precleared with protein A/G plus- agarose beads (Santa Cruz Biotechnology), G sepharose and A sepharose (GE Healthcare) as indicated and then incubated at 4^{o}C for 3 h. If DNase1 or ethidium bromide was used, the whole cell lysates were either treated with 100 mg/ml DNase1 (Invitrogen) for 20 min at 37^{o}C or 50mg/ml ethidium bromide (Sigma) on ice for 30 min. Next, the appropriate antibody was added, and incubated at 4^{o}C for 12 h. After the addition of fresh protein A/G plus-agarose bead, G sepharose and A sepharose, the reaction was incubated overnight at 4^{o}C with rotation. The beads were washed five times in RIPA buffer without protease inhibitors, resuspended in SDS sample buffer and boiled for 5 min. The samples were then analyzed by western blotting using the appropriate antibodies.

G. Immunostaining

To visualize γ-ray- or NCS-induced foci, untreated cells or cells treated with 100 ng/ml NCS were cultured on coverslips coated with poly-L-lysine (Sigma). Cells were washed twice with PBS and fixed in 98% methanol for 10 min, followed by permeabilization with 0.3% Triton X-100 for 15 min at room temperature. Next, the coverslips were washed three times with PBS, followed by blocking with 0.1% bovine serum albumin in PBS for 1 h at room temperature. The cells were double-immunostained using primary antibodies directed against the indicated proteins overnight at 4^{o}C. The cells were then washed with PBS and stained with the appropriate Alexa Fluor 488- or Alexa Fluor 594-conjugated secondary antibodies (green and red fluorescence, respectively; Molecular Probes, Eugene, OR, USA). After washing, the coverslips were mounted onto slides using Vectashield mounting medium containing 4, 6-diamidino-2-phenylindole (DAPI; Vector Laboratories, Burlingame, CA, USA). Fluorescence images were taken under a confocal microscope (Zeiss LSM 510 Meta; Carl Zeiss, Jena, Germany) and analyzed with Zeiss LSM Image Examiner software (Carl Zeiss). For foci quantification experiments, cells with ≥10 foci were counted as MSH6 or γ-H2AX foci-positive cells and the percentage was calculated among at least 100 cells by dividing the number of MSH6 or γ-H2AX foci-positive cells by the number of DAPI-stained cells. The error bars represent standard error in three independent experiments.

H. Cell survival assay

After treatment with NCS or IR, 5 ×10^{2} cells were immediately seeded onto a 60-mm dish in duplicate and grown for 2–3 weeks at 37^{o}C to allow colony

formation. Colonies were stained with 2% methylene blue in 50% ethanol and counted. The fraction of surviving cells was calculated as the ratio of the plating efficiencies of treated cells to untreated cells. Cell survival results are reported as the mean value ± standard deviation for three independent experiments.

I. Comet assay

DSB repair was assayed by alkaline single-cell agarose-gel electrophoresis as described previously. Briefly, control and MSH6-knockdown cells were treated with 100 ng/ml NCS or 5 Gy of γ-ray followed by incubation in culture medium at 37^{o}C for the indicated times. Cells were then harvested (~10^5 cells per pellet), mixed with low-melting temperature agarose, and layered onto agarose-coated glass slides. The slides were maintained in the dark at 4^{o}C for all of the remaining steps. Slides were submerged in lysis solution [10mM Tris–HCl (pH 10), 2.5M NaCl, 0.1M EDTA, 1% Triton X-100, 10% dimethyl sulfoxide] for 1 h and incubated for 30 min in alkaline electrophoresis solution (300mM NaOH, 200mM EDTA at pH >13). After electrophoresis (~30 min at 1 V/cm tank length), air-dried and neutralized slides were stained with 30– 50 ml ethidium bromide (20 mg/ml). Average comet tail moment was scored for 40–50 cells/slide using a computerized image analysis system (Komet 5.5; Andor Technology, South Windsor, CT, USA).

J. Analysis of NHEJ activity

To analyze the role of MSH6 in NHEJ in vivo, we used the pEGFP-Pem1-Ad2 system (26). The plasmid was digested with HindIII to remove Ad2 and generate different types of ends. Supercoiled pEGFP-Pem1 was used as a positive control for standardization of transfection and analysis conditions. The pCMV-dsRed-express

plasmid (Clontech) was co-transfected with either linearized pEGFP-Pem1-Ad2 or supercoiled pEGFP-Pem1 as a control for transfection efficiency. In a typical reaction, 5×10^5 cells were transfected with 0.5 μg of linearized pEGFP-Pem1-Ad2 or 0.5 μg supercoiled pEGFP-Pem1, together with 0.5 μg of pDsRed2-N1 plasmid, using Lipofectamine 2000 (Invitrogen) according to the manufacturer's recommended protocol. Twenty-four hours after transfection, green (EGFP) and red (DsRed) fluorescence was measured by flow cytometry (FACSCalibur; BD Biosciences, San Jose, CA, USA).

K. Statistical analysis

Data are presented as means ± SD. Statistical comparisons were carried out using unpaired *t*- tests, and values of $P<0.01$ were considered to be statistically significant.

III. RESULTS

A. Interaction of Ku70 and MSH6

To search for factors that interacts with Ku70, yeast two- hybrid screening of a human prostate cDNA library was performed using full length human Ku70 as bait. One of the positive clones isolated from 2×10^6 transformants turned out to be MSH6. Human MSH6 could also interact with human Ku70 was confirmed by performing the yeast two hybrid assays with a human MSH6 cDNA. To generate MSH6 cDNA, MUSTd domain of MSH6 (GenBank accession number NM_000179.2) containing residues 2257-3297 was extracted from the NCBI Entrez nucleotide database. The transformed colonies showed the ability to grow in medium lacking adenosin, histidine, tryptophan and leucine (-AHLT) and to turn blue in a β-galactosidase assay, while cells contransformed with the control vector pGBT9 vector did not do so with a construct containing the human MSH6 cDNA (Figure 4).

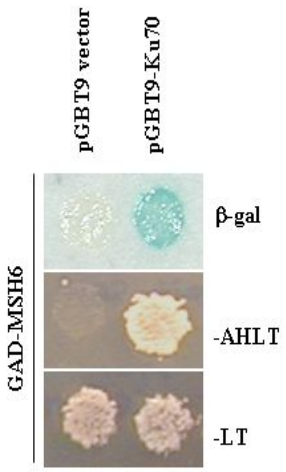

Figure 4 Protein interaction study by Yeast two Hybridization assay

Yeast cells were co-transfected with the GAD-MSH6 and pGBT9 control vector or pGBT9-Ku70 (full length). Co-transformants were plated on selection plates lacking leucine and tryptophan (-LT) (bottom panel) or lacking adenine, histidine, leucine, and tryptophan (-AHLT) (middle panel). Growth was recorded after 72 h. For the β-galatosidase assay, filter lift assays were performed. Blue indicates specific interaction of two proteins (upper panel, second lane).

B. Endogenous binding of Ku70 and MSH6 upon DNA damage

To determine whether Ku70 interacts with MSH6 in human cells endogenously expressing both proteins, immunoprecipitation assays was performed. For production of DSBs, HeLa cells were treated with 100 ng/ml of the radiomimetic drug NCS or 5 Gy of IR. The cells were then lysed, and endogenous MSH6 was immunoprecipitated with a MSH6-specific antibody. Immunoprecipitates were subjected to western blotting with an anti-Ku70 antibody. Immunoprecipitation with anti-MSH6 antibodies revealed that endogenous MSH6 bound Ku70 and that treatment with NCS or IR increased the amount of MSH6 bound to Ku70 (Figure 5A). In this reciprocal experiments, Ku70 antibody was able to coimmunoprecipitate MSH6 (Figure 5B), suggesting that these proteins may interact with each other directly or indirectly in cells. As control, normal rabbit IgG did not coimmunoprecipitate Ku70 or MSH6, indicating that the coimmunoprecipitation of Ku70 with MSH6 was not due to non-specific antibody binding. Because the MSH6 protein is complexed with MSH2 to form the MutS a heterodimer (Gradia et al., 1997), whether Ku70 interacts with MSH2, was tested. When proteins were immunoprecipitated with anti-Ku70 and then probed with anti-MSH2, MSH2 was detected (Figure 5B, second panel).

To further document, the physiological relevance of the interaction, whether MSH6 interacts with other components of the NHEJ system by coimmunoprecipitation assays, was investigated. NHEJ is initiated by binding of the Ku70/86 heterodimer to both ends of the broken DNA molecule, and this step is essential for recruitment of DNA-PK_{CS} (Lieber et al., 2003). The assembled DNA-PKcs then exhibits serine-threonine protein kinase and DNA end-bridging activities

(Collis et al., 2005). Finally, the XRCC4/DNA ligase IV complex is responsible for the ligation step (Li et al., 1995; Grawunder et al., 1998). Endogenous MSH6 and Ku86 could be coimmunoprecipitated by anti-MSH6 antibodies (Figure 5C, second panel), but not by control IgGs, and this was increased after treatment of NCS. Whether MSH6 binds DNA-PK_{CS} or XRCC4 in human cells, was then tested. Immunoprecipitation of lysates using anti-MSH6 antibodies revealed that endogenous MSH6 and DNAPKcs did not interact in the absence of NCS, but upon NCS treatment the interaction was found (Figure 5C, third panel). However, interaction between MSH6 and XRCC4 in the presence of NCS was not detected by coimmunoprecipitation (Figure 5C, fourth panel).

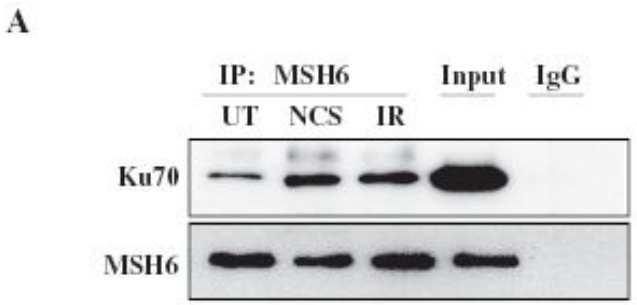

Figure 5 DNA damage stimulates interaction of MMR protein MSH6 with Ku70
(A) HeLa cells were untreated (UT) or treated with 100 ng/ml NCS or 5Gy ionizing radiation (IR). Proteins were immunoprecipitated (IP) from the lysates using an anti-MSH6 antibody 3 h after treatment. Immunoprecipitates were then subjected towestern-blot analysis using antibodies specific for Ku70 or MSH6. The fourth lane contains 5% input for Ku70 and 20% input for MSH6. Normal rabbit IgG was used for negative control immunoprecipitations

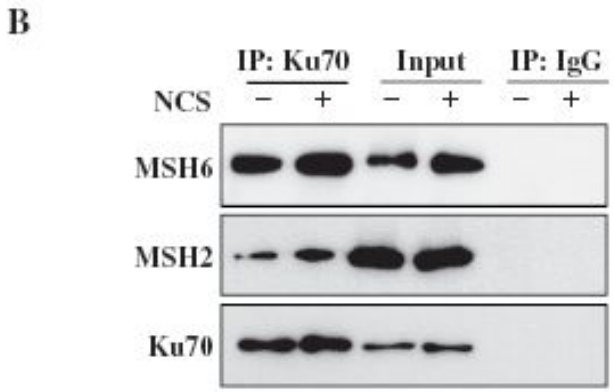

Figure 5 Ku70 interacts with MSH6 and MSH2 after NCS- induced DNA damage. (B) HeLa cells were untreated or treated with 100 ng/ml NCS for 3 h. Proteins were immunoprecipitated from the lysates using an anti-Ku70 antibody. Immunoprecipitates were then subjected to western-blot analysis using antibodies specific for MSH6, MSH2 or Ku70. The third and fourth lane contains 5% input for Ku70 and 20% input for MSH6 and MSH2. Normal rabbit IgG was used for negative control immunoprecipitations.

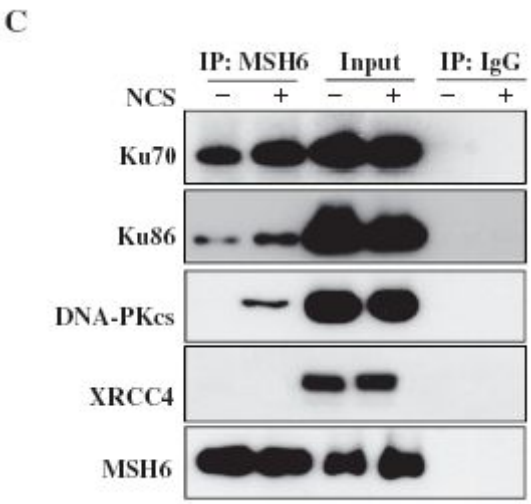

Figure 5 MSH6 also interacts with Ku70, Ku86, DNA-PKcs and XRCC4 after DNA damage (C) HeLa cells were untreated or treated with 100 ng/ml NCS for 3 h. Proteins were immunoprecipitated from the lysates using an anti-MSH6 antibody.

Immunoprecipitates were then subjected to western-blot analysis using antibodies specific for Ku70, Ku86, DNA-PKCS, XRCC4 or MSH6. The third and fourth lane contains 5% input for Ku70 and 20% input for Ku86, DNA-PKcs, XRCC4 and MSH6. Normal rabbit IgG was used for negative control immunoprecipitations.

Next the binding kinetics of MSH6 and Ku70 at different time periods after treatment with NCS was investigated. Immunoprecipitation analysis revealed that the level of interaction between the two proteins clearly increased by 3 h after NCS treatment and further increased by 6 h after treatment, then decreased in a time-dependent manner (Figure 5D). These observations indicate that Ku70 and MSH6 complex formation increases at the early onset of DSB formation and dissociates at later time points.

D

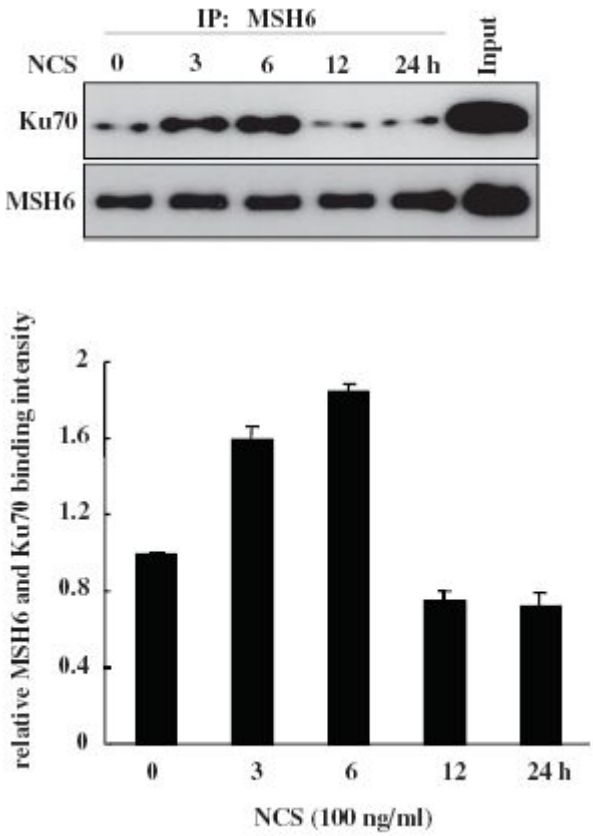

Figure 5 Time dependent binding assay of MSH6 and Ku70

(D) HeLa cells were untreated or treated with 100 ng/ml NCS, and cells were lysed at the indicated times. Whole-cell lysates were subjected to immunoprecipitation using an anti-MSH6 antibody, and the resulting immunoprecipitates were subjected to western-blot analysis using anti-Ku70 and anti-MSH6 antibodies. Graphs show the quantification of the level of Ku70. The sixth lane contains 5% input for Ku70 and 20% input for MSH6. The data were normalized to the untreated control (as the value of 1) and are the mean ± SD of three independent experiments.

C. DNA is not required for Ku70 association with MSH6

Since both MSH6 and Ku70 are chromatin-bound proteins in cells, we considered the possibility that the interaction between MSH6 and Ku70 was mediated by the independent binding of both protein complexes to DNA. To exclude this possibility, we pretreated cell lysates with DNase I, or ethidium bromide (EtBr), which is known to disrupt protein–DNA interactions, prior to coimmunoprecipitation. Our data showed that DNA did not mediate MSH6-Ku70 association (Figure 6). These results suggested that MSH6 forms a physiological complex with Ku heterodimer in vivo.

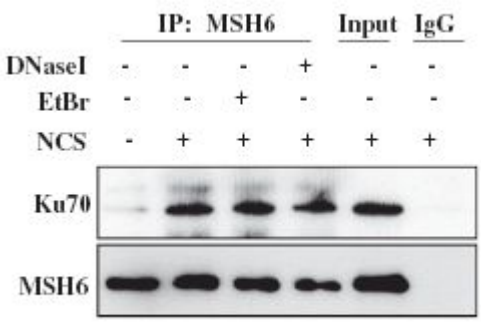

Figure 6 The interaction of MSH6 and Ku70 is not mediated via DNA-protein interation and is not sensitive to DNA disrupting agents. HeLa cells were untreated or treated with 100 ng/ml NCS for 3 h. Whole cell lysates were treated with 50 mg/ml ethidium bromide (EtBr) on ice for 30 min (lane 3) or 100 mg/ml DNase I for 20 min at 37^{o}C (lane 4) or mock-treated (lane 2). Cell lysates were then subjected to coimmunoprecipitation assays with MSH6 antibody and detected by anti-Ku70 or anti-MSH6. The fifth lane contains 5% input for Ku70 and 20% input for MSH6.

D. Interaction of full length MSH6 and Ku70

To further confirm this interaction, HEK293T cells were transiently transfected with an expression construct encoding full-length Ku70 tagged with HA and a second construct that expressed full-length MSH6. Co-immunoprecipitation assays were then performed using an MSH6-specific antibody for immunoprecipitation and an anti-HA antibody for immunoblotting. Immunoprecipitation with the anti-MSH6 antibody revealed that MSH6 was associated with HA-tagged, full-length Ku70 in both control and NCS-treated cells and that the level of binding increased after NCS treatment (Figure 7). Therefore, it is likely that MSH6 forms a complex with Ku70. In spite of this, it remains possible that other proteins may mediate the interaction between MSH6 and Ku70 complex because both complexes possess a variety of interacting partners.

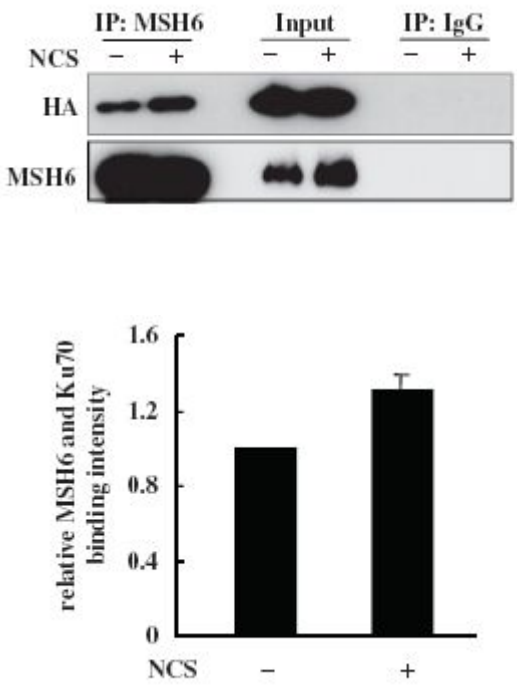

Figure 7 Exogenous binding of full length MSH6 with HA- tagged Ku70

HEK293T cells were transfected with full-length MSH6 and HA-tagged Ku70 expression vectors. After 24 h, cells were untreated or treated with 100 ng/ml NCS for 3 h. Proteins were immunoprecipitated from HEK293T cell lysates using an anti-MSH6 antibody, and the resulting immunoprecipitates were subjected to western-blot analysis using anti-HA or anti-MSH6 antibodies. Graphs show the quantification of the level of HA-Ku70. The third and fourth lane contains 20% input. The data were normalized to the untreated control (as the value of 1) and are the mean ± SD of three independent experiments.

E. MSH6 forms nuclear foci and colocalizes with γ -H2AX in response to DNA damage

After DNA damage, many DNA-damage-repair proteins are recruited to the DNA-damage sites and form discrete DNA-damage-induced nuclear foci. The order and timing of these events are thought to be critical for DNA repair (Stewart et al., 2003). Thus, it was interesting to investigate whether MSH6 also forms NCS- or IR-induced nuclear foci. In untreated HeLa cells, anti-MSH6 antibody staining yielded diffuse nuclear staining (Figure 8A and B). Numerous nuclear foci were apparent in cells 1 h after 100 ng/ml NCS treatment (Figure 8A). MSH6 foci were also evident in HeLa cells 30 min after irradiation at 5 Gy (Figure 8B). MSH6 foci peak at 6 or 12 h after NCS or IR treatment, respectively, and then significantly declined. Immunofluorescence staining was also carried out to check whether Ku70 could form nuclear foci after NCS treatment. However, Ku70 did not form nuclear foci. Ku70 staining in NCS- or IR-treated cells was weak and diffused throughout the nucleus (Figure 9).

A

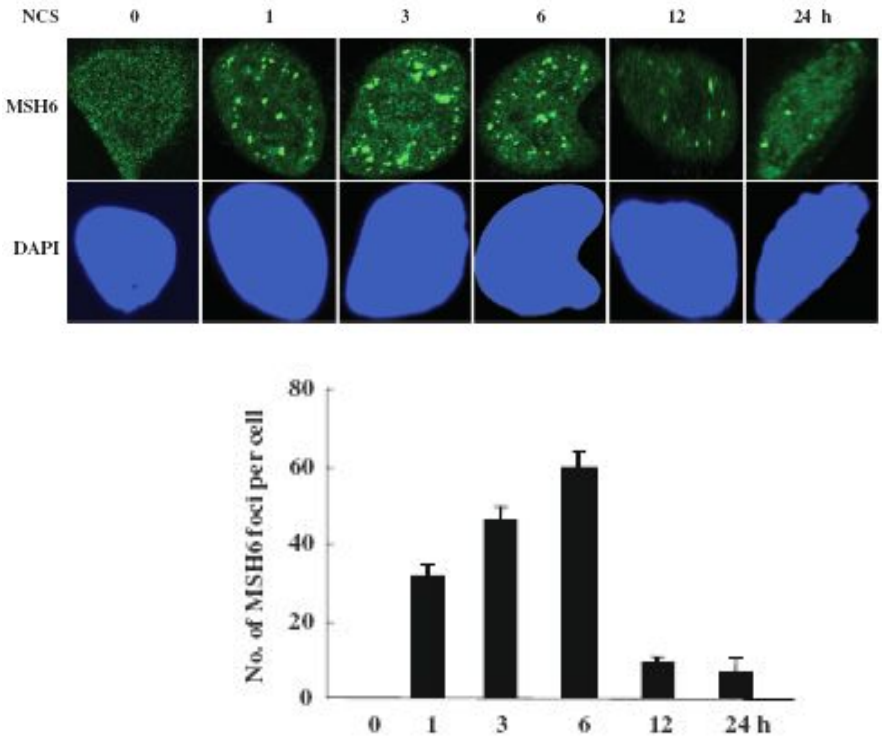

Figure 8 Foci formation of MSH6 near DSB site upon NCS treatment

(A) HeLa cells were untreated or treated with 100 ng/ml NCS. At the indicated times, cells were fixed and immunostained using an anti-MSH6 antibody. Representative cells containing foci are shown. Nuclei were stained with DAPI. The number of MSH6 foci ('Materials and Methods' section) determined by confocal microscopy ($N = 3$).

B

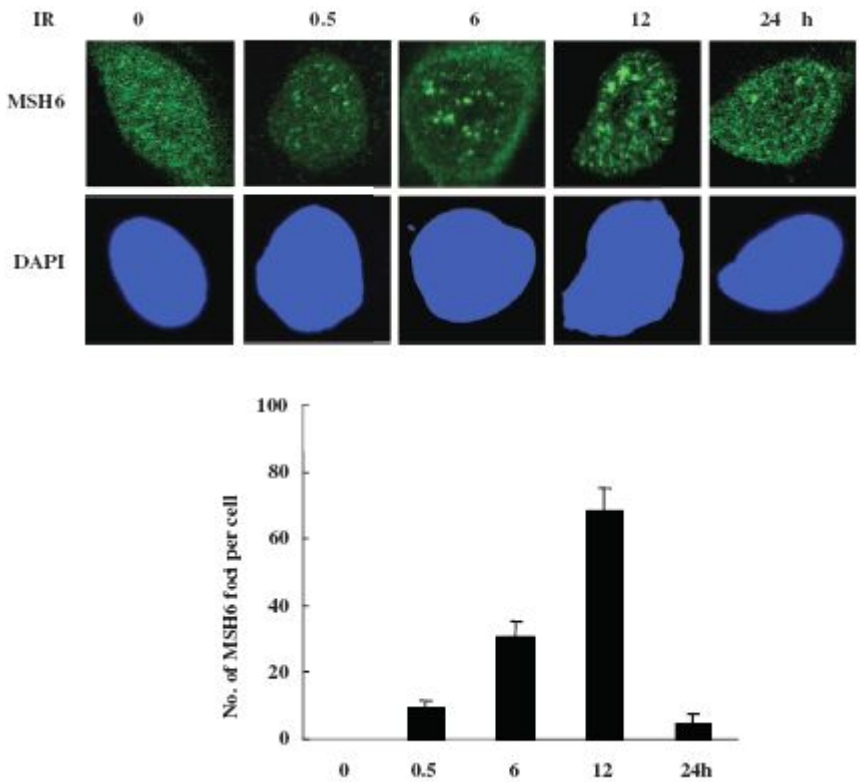

Figure 8 Foci formation of MSH6 near DSB site in response to IR

(B) HeLa cells were untreated or treated with 5Gy ionizing radiation (IR). At the indicated times, cells were fixed and immunostained using an anti-MSH6 antibody. Representative cells containing foci are shown. Nuclei were stained with DAPI. The number of MSH6 foci ('Materials and Methods' section) determined by confocal microscopy ($N = 3$).

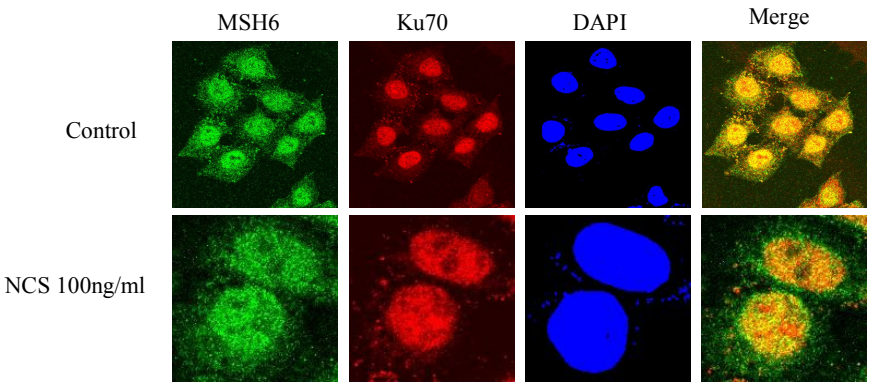

Figure 9 Colocalization of MSH6 and Ku70 upon DNA damage

HeLa cells were left untreated or treated with neocarzinostatin (NCS) (100 ng/ml), fixed at the indicated time points and immunofluorescence analysis with antibody against MSH6 and Ku70 were carried out. 40-6-Diamidino-2-phenylindole (DAPI) staining was performed to indicate the positions of nuclei. At least 100 cells were analyzed for each treatment.

γ- H2AX focus formation on the DSB sites is one of the earliest events in response to forms of DNA damage that induce DSBs (Rogakou et al., 1998). Based on above observations, the potential colocalization of MSH6 and γ-H2AX into the same nuclear foci was investigated after DNA damage. Thus, the immunofluorescent staining analysis was conducted. As shown in Figure 10A, MSH6 in the mock-treated cells appears to be homogenously distributed through the nucleus and γ -H2AX foci was not found. Upon NCS or IR treatment, a clear redistribution of MSH6 and γ -H2AX to form discrete nuclear foci was occurred (Figure 10A and B). Some extent of colocalization of these foci occurred. Such limited degree of colocalization was probably reflecting the fact that both MSH6 and γ-H2AX are able to interact with several protein partners and function in

multiple biological pathways in cells. A quantitative assessment made on MSH6 and γ -H2AX colocalization by counting all of the foci in at least 50 randomly chosen untreated and NCS- or IR-treated cells is given in Figure 8A and B, lower panel. The analysis revealed that ~50% of MSH6 foci coincided with that of γ -H2AX 3 or 6 h after 100 ng/ml NCS or 5 Gy IR treatments, respectively. These results suggest that MSH6 may relocalize to the same DSB site as γ -H2AX after DNA damage.

A

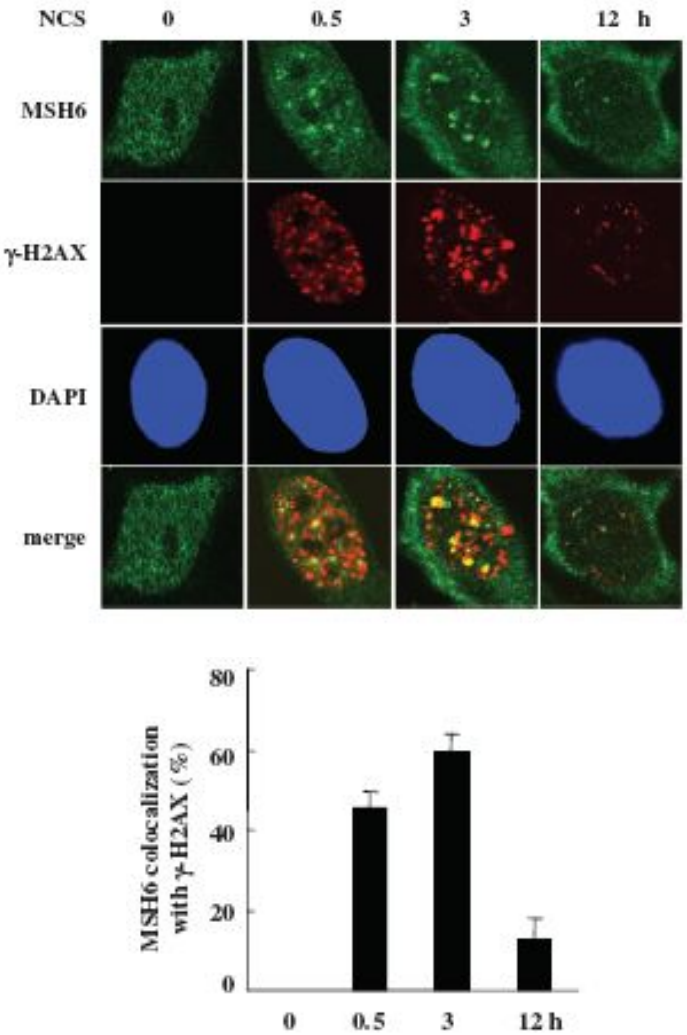

Figure 10 Colocalization of MSH6 and γ-H2AX near DSB site after NCS treatment. (A) HeLa cells were untreated (UT) or treated with 100 ng/ml NCS and fixed for the indicated time points after NCS. Colocalization of endogenous MSH6 and γ -H2AX was detected using antibodies specific for MSH6 and γ -H2AX. MSH6 and γ –H2AX antibodies were visualized with Alexa Fluor 488- or Alexa Fluor 546-conjugated secondary antibodies, respectively, followed by confocal

microscopy. Colocalization of MSH6 (green) and Ku70 (red) in cells appears yellow in merged images. Graph showing the Quantification of the percentage of colocalizing foci between MSH6 and γ- H2AX. An average of 50 merged nuclear foci from three independent slides was analyzed for each time point.

B

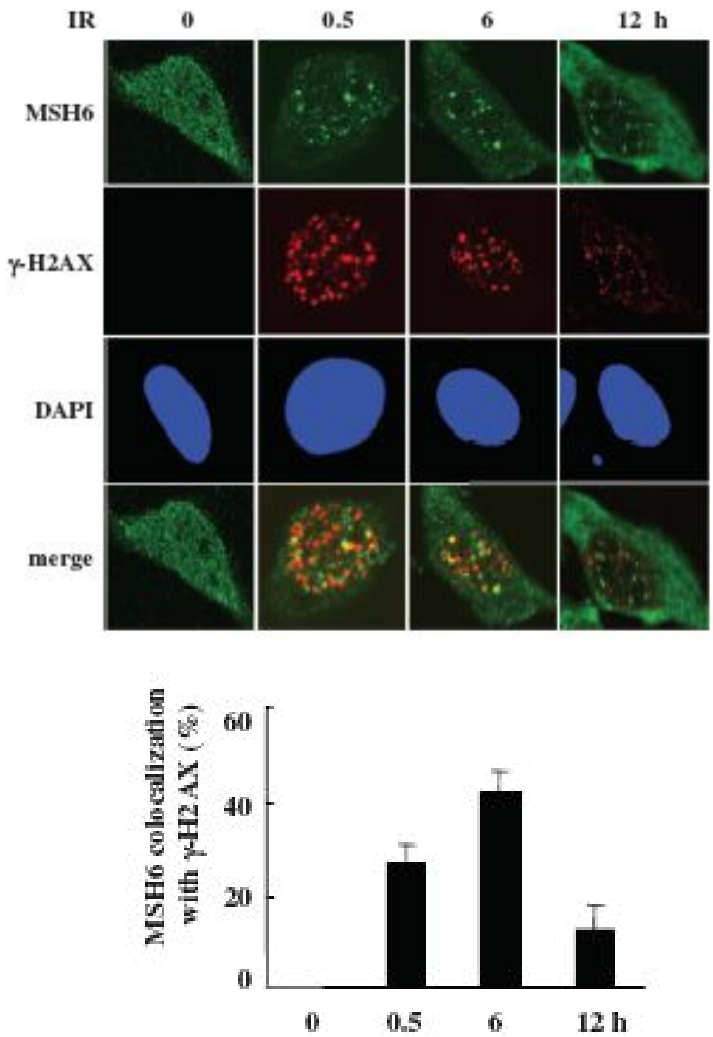

Figure 10 Colocalization of MSH6 and γ-H2AX near DSB site after IR treatment (B) HeLa cells were untreated (UT) or treated with 5Gy ionizing radiation (IR) and fixed for the indicated time points after IR treatment. Colocalization of endogenous MSH6 and γ -H2AX was detected using antibodies specific for MSH6 and γ -H2AX. MSH6 and γ -H2AX antibodies were visualized with Alexa Fluor 488- or

Alexa Fluor 546-conjugated secondary antibodies, respectively, followed by confocal microscopy. Colocalization of MSH6 (green) and Ku70 (red) in cells appears yellow in merged images. Graph showing the Quantification of the percentage of colocalizing foci between MSH6 and γ- H2AX. An average of 50 merged nuclear foci from three independent slides was analyzed for each time point.

F. MSH6 knockdown suppresses NHEJ

To investigate the biological significance of the MSH6/ Ku70 interaction, the role of MSH6 in NHEJ was assessed. The pEGFP–Pem1–Ad2 system and short hairpin RNA (shRNA)-mediated depletion was combined to analyze the effects of MSH6 knockdown on the efficiency of NHEJ after formation of DSBs. The reporter cassette for detection of NHEJ activity was previously described (Kang et al., 2009). The principal characteristic of the plasmid (pEGFP– Pem1–Ad2) used in this assay (Figure 11A) is the interruption of the EGFP sequence by a 2.4-kb intron derived from the rat Pem1 gene. An exon derived from adenovirus (Ad) was introduced into the middle of the intron, and it was flanked on both sides by HindIII restriction enzyme recognition sequences. In undigested or partially digested plasmids, GFP is not expressed because the Ad exon is efficiently incorporated into the GFP mRNA. However, when the plasmid is linearized by HindIII digestion, the Ad2 exon is removed, enabling expression of EGFP upon successful intracellular recircularization. EGFP expression can then be easily detected and quantified by flow cytometry. Transfection with the supercoiled pEGFP– Pem1 plasmid is used to evaluate EGFP-signal expression without the requirement for rejoining, and the pCMVdsRed express plasmid is used as a control to determine transfection efficiency for this assay.

A

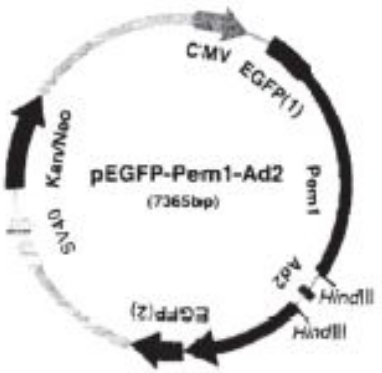
CMV
EGFP(1)
Perm1
Ad2
HindIII
HindIII
EGFP(2)
SV40
Kan/Neo
pEGFP-Perm1-Ad2
(7365bp)

B

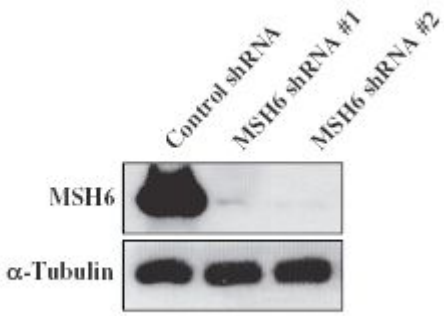
Control shRNA
MSH6 shRNA #1
MSH6 shRNA #2
MSH6
α-Tubulin

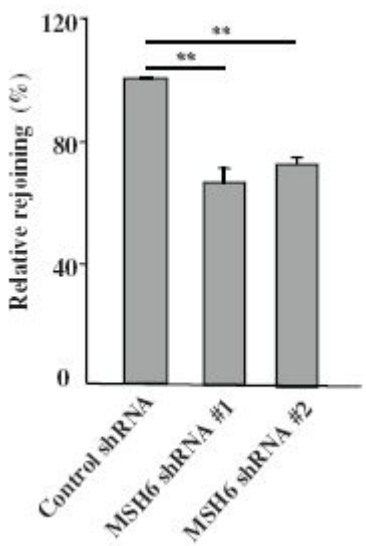
120
80
40
0
Relative rejoining (%)
**
**
Control shRNA
MSH6 shRNA #1
MSH6 shRNA #2

Figure 11 MSH6 contributes to DNA end joining *in vivo* (A) Map of the pEGFP–Pem1–Ad2 vector. The reporter substrate consists of the GFP gene under control of the CMV promoter. The GFP gene contains an engineered intron from the rat Pem1 gene, which is interrupted by an adenoviral exon (Ad) that is flanked by HindIII recognition sites. In this construct, the GFP gene is inactive; however, after digestion with HindIII and successful NHEJ, the construct expresses GFP. (B) HeLa cells were transfected with control or one of two different MSH6 shRNA expression vectors (MSH6 shRNA #1 and #2) and selected with 400 µg/ml G418. Four weeks later, the expression level of the MSH6 protein was determined by immunoblot analysis using an anti-MSH6 antibody. Control and MSH6-knockdown HeLa cells were transfected with supercoiled pEGF–Pem1 or HindIII-linearized pEGFP– Pem–Ad2 together with pCMV-dsRed-express. To quantify NHEJ events, the cells were analyzed by flow cytometry 24 h after transfection. DsRed expression was used to normalize transfection efficiency. The ratio of GFP-positive (GFP^+) to DsRed-positive ($DsRed^+$) cells was used as a measure of NHEJ. Relative levels of plasmid rejoining compared to control shRNA-transfected cells were calculated by dividing the GFP^+/ $DsRed^+$ ratios of the samples and plotted. Means are representative of at least three independent experiments. Error bars indicate the SD. Asterisk denotes $P<0.01$.

To determine whether MSH6 plays a role in regulation of NHEJ activity, firstly, MSH6 was silenced in HeLa cells using plasmid-mediated shRNA expression technology to create stable MSH6 knockdown cell lines (MSH6 shRNA #1 and MSH6 shRNA #2). Immunoblotting confirmed that expression of endogenous MSH6 was reduced by more than 90% in both cell lines stably transfected with the two different MSH6 shRNAs in comparison to control shRNA-transfected cells (Figure 11B). To evaluate the efficiency of NHEJ, MSH6 knockdown cells (MSH6

shRNA #1 and MSH6 shRNA #2) were transfected with either linearized pEGFP–Pem1–Ad2 or supercoiled pEGFP–Pem1 together with pDsRed2–N1. The cells were then incubated for 24 h to allow expression of EGFP (green) and DsRed (red), followed by flow cytometry analysis. To control for the efficiency of transfection, the ratio of GFP+ cells to DsRed+ cells was used as the normalized measure of NHEJ efficiency. As shown in Figure 9B, lower panel, NHEJ activity decreased significantly in both MSH6-depleted cell lines in comparison to control cells. In three independent experiments, the average NHEJ efficiency was 66.11±4.95% in the MSH6 shRNA #1 cells and 72.81±2.44% in the MSH6 shRNA #2 cells relative to control shRNA- transfected cells. These results indicate that MSH6 contributes to DSB repair through regulation of NHEJ.

G. MSH6 expression stimulates NHEJ

The reduced NHEJ activity present in cells depleted of MSH6 raised the possibility that restoration of MSH6 in MMR-deficient cells may increase NHEJ activity. To assess this possibility, the human colon cancer cell line DLD1 was utilized, which is deficient for MSH6 (Papadopoulos et al., 1995). DLD1 cells were transiently transfected with the pCMV6- hMSH6 vector, which drives expression of full-length MSH6, or with the control pCMV6 vector. Western-blot analysis confirmed that MSH6 was highly expressed 24 h after transfection with the pcDNA3–MSH6 plasmid (Figure 12). MSH6-expressing cells were then transfected with either linearized pEGFP–Pem1– Ad2 or supercoiled pEGFP–Pem1 together with pDsRed2–N1, and the numbers of red and green fluorescent cells were quantified by FACS after 24 h. Introduction of the HindIII-linearized pEGFP–Pem1–Ad2 plasmid into MSH6-expressing DLD1 cells revealed an ~50% increase

in NHEJ activity in comparison to control DLD1 cells (Figure 12, lower panel). These results indicate that MSH6 is involved in regulation of the NHEJ pathway for repair of DSBs.

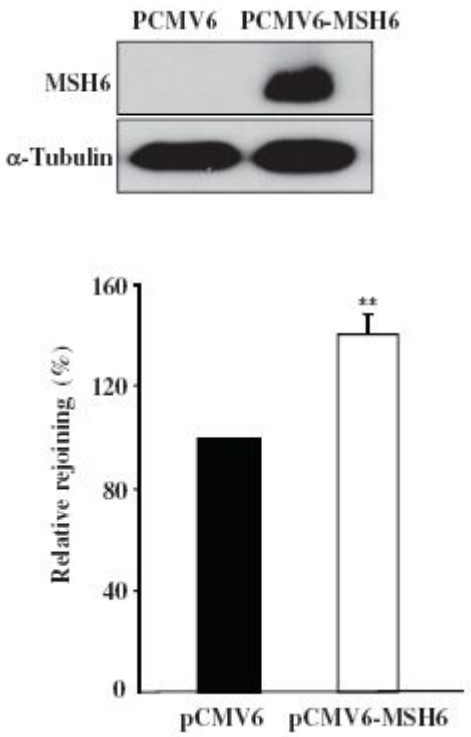

Figure 12 over-expression of MSH6 significantly increases NHEJ activity

DLD1 cells were transiently transfected with either the control vector (PCMV6) or an MSH6 expression vector (pCMV6–MSH6). The level of MSH6 expression in rescued cells was analyzed by western blotting using an antibody specific for MSH6. Quantitative analysis considering signal intensity of the α-Tubulin loading control gives for this experiment an over-expression effect of 90%. NHEJ in control and MSH6-expressing DLD1 cells was measured using the pEGFP–Pem–Ad2

system. Means are representative of at least three independent experiments. Error bars indicate the S.D. Asterisk denotes P<0.01.

H. MSH6 knockdown delays DNA DSB repair

To further address whether MSH6-deficient cells exhibit defects in rejoining DNA DSBs, the formation of γ-H2AX foci was analyzed. One of the primary responses to the formation of DSBs is phosphorylation of the histone variant H2AX at Ser193 (Rogakou et al., 1998). Levels of phosphorylated H2AX (γ -H2AX) and quantitative analysis of γ -H2AX foci following IR are often used as measures of DSB induction and the efficiency of DNA repair. Therefore, whether MSH6 knockdown affected the formation of γ -H2AX foci by immunofluorescence microscopy after NCS (Figure 13 A and B) or IR treatment (Figures 13C) was investigated. In control cells, the maximum numbers of γ-H2AX foci were observed ~1 h after treatment with 100 ng/ml NCS (Figure 13B) or 5 Gy IR (Figure 13C).

Longer recovery times resulted in a decline in the numbers of γ -H2AX foci. By 6 h after NCS or IR treatment, γ -H2AX foci were significantly decreased, indicating that the NCS- or IR-induced DSBs were almost repaired. In contrast, although the formation of γ -H2AX foci was similar in control and in MSH6-deficient cells up to 30 min after NCS or IR treatment, γ -H2AX foci persisted for longer time periods in MSH6-knockdown cells compared to control cells. MSH6-knockdown cells contained a significant amount of γ -H2AX nuclear foci even at 6 h after NCS or IR treatment.

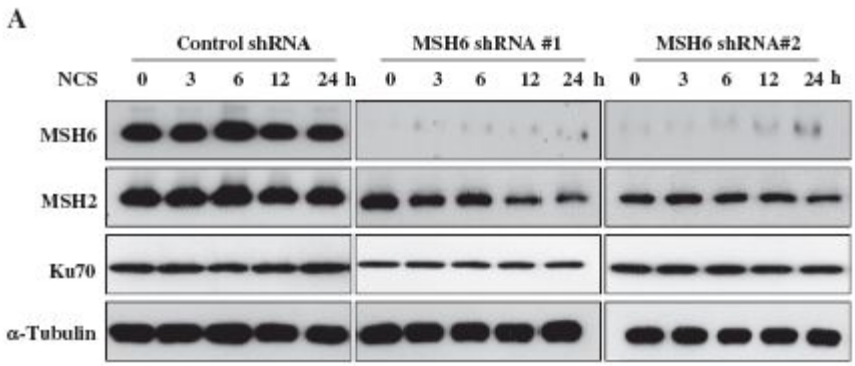

Figure 13 The protein level of MSH6, Ku70 and MSH2 in stably knockdown cell (A) Control and MSH6-depleted HeLa cells were untreated (0 min) or treated with 100 ng/ml NCS. Whole-cell lysates were prepared at the indicated time points, and western-blot analysis was performed using specific antibodies directed against MSH6, MSH2, Ku70 and α-tubulin.

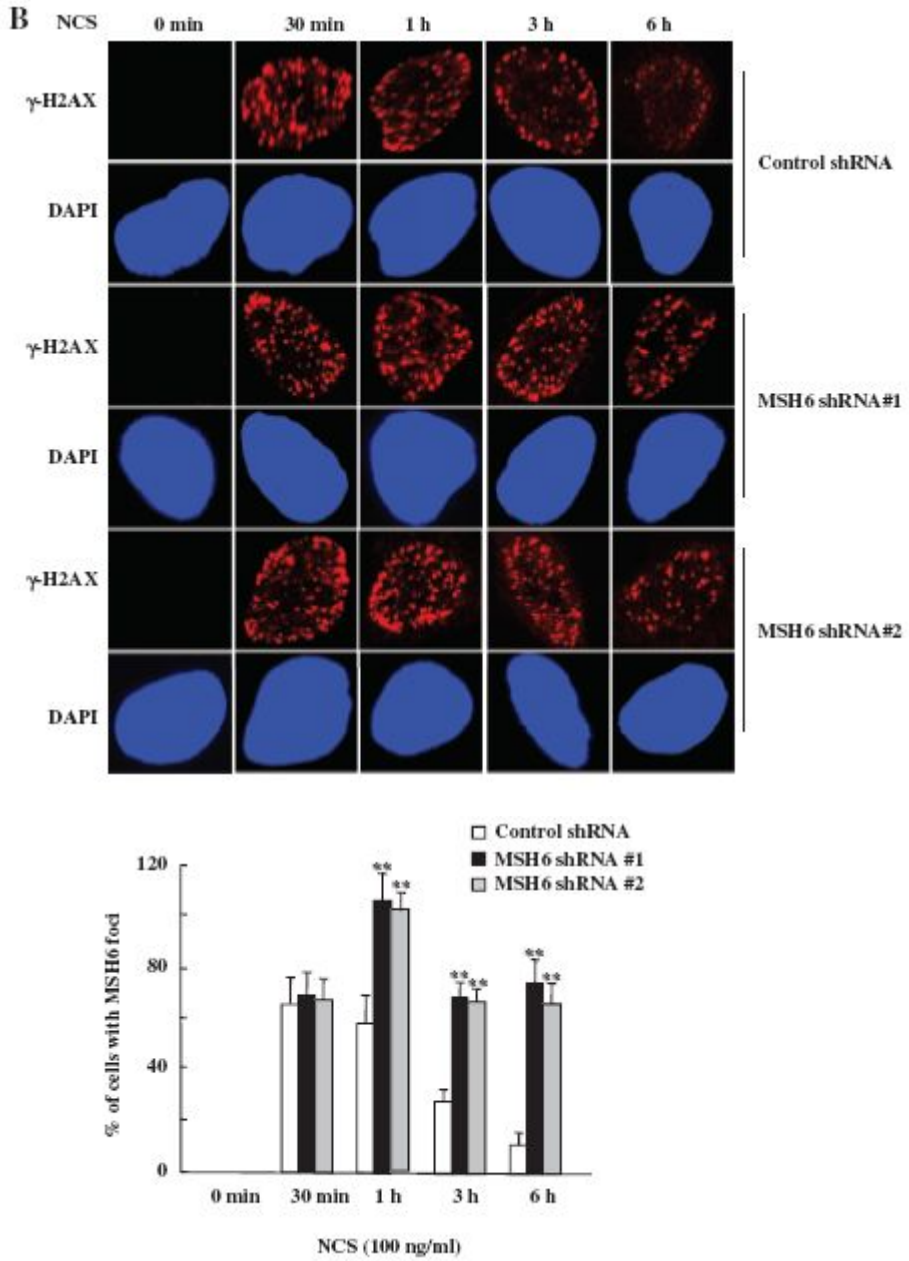

Figure 13 MSH6-deficient cells exhibit prolonged γ-H2AX staining after NCS treatment.

(B) Control and MSH6-depleted HeLa cells were untreated or treated with 100 ng/ml NCS and were then fixed at the indicated times. Cells were stained with an anti-γ-H2AX antibody and the DNA was counterstained using DAPI. The percentage of γ-H2AX foci positive cells determined by confocal microscopy (*N*=3). Error bars represent the mean ±SD. Asterisk denotes P<0.01.

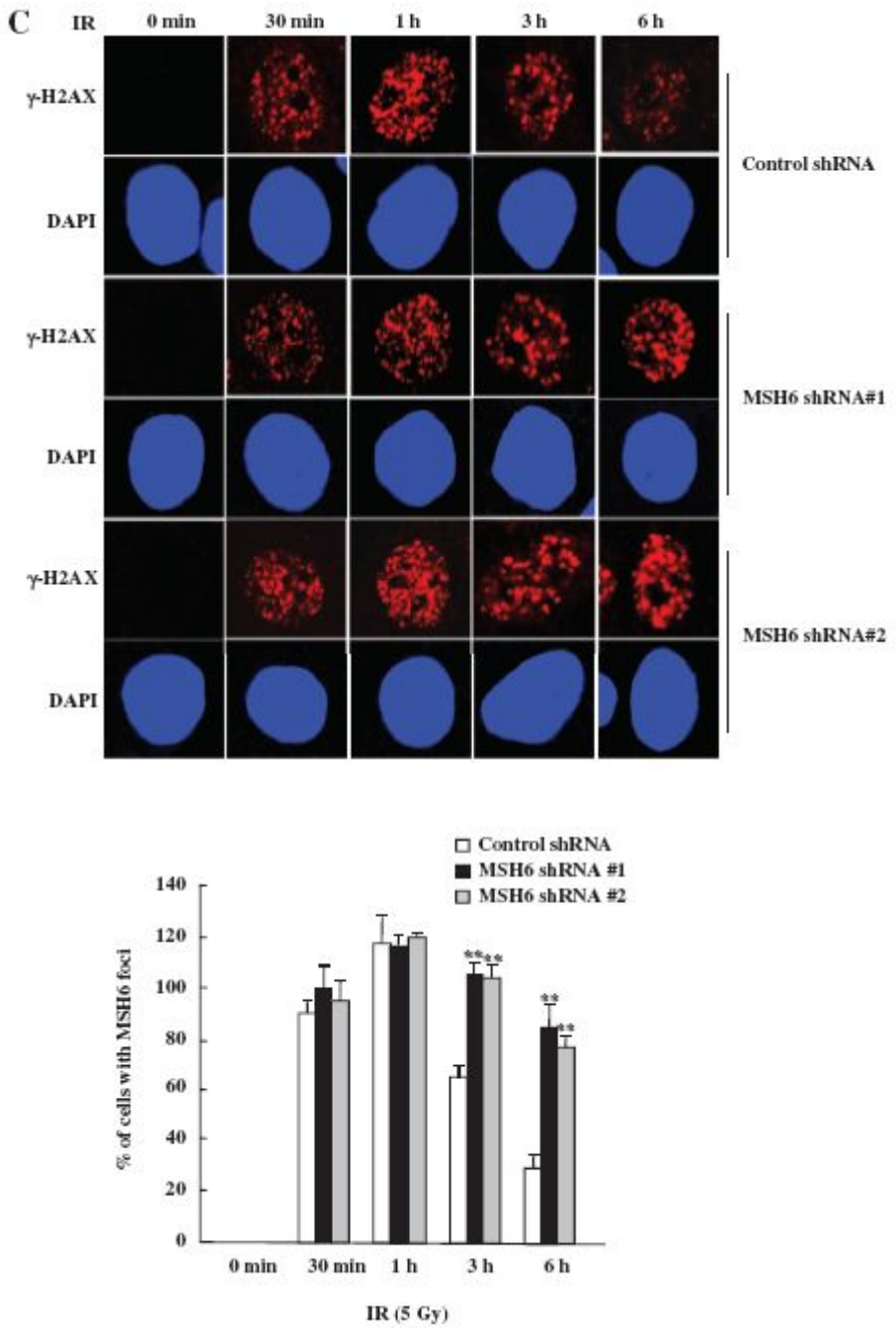

Figure 13 MSH6-deficient cells exhibit prolonged γ-H2AX staining after IR treatment. (C) Control and MSH6-depleted HeLa cells were untreated or treated

with 5 Gy ionizing radiation and were then fixed at the indicated times. Cells were stained with an anti-γ-H2AX antibody and the DNA was counterstained using DAPI. The percentage of γ-H2AX foci positive cells determined by confocal microscopy (*N*=3). Error bars represent the mean ±SD. Asterisk denotes P<0.01.

I. Depletion of MSH6 inhibits DNA double-strand break (DSB) repair and sensitizes cells to DNA damaging agent

To confirm these results, the persistence of DSB was measured in NCS- or IR-treated HeLa cells stably transfected with MSH6 or control shRNA by single-cell electrophoresis (the comet assay). This very sensitive method can be used to detect low levels of DNA breaks. NCS or IR treatment induces DSBs, visible as increased DNA mobility or 'comet tails'. At 30 min after NCS or IR treatment, control and MSH6-knockdown cells exhibited comparable levels of DNA damage. However, when the persistence of unrepaired DNA-strand breaks was analyzed at a various times after NCS or IR treatment, cells depleted of MSH6 exhibited significantly lower repair efficiency than control cells (Figure 14A and B). Based on the comet tail moments, which quantify the extent of

DNA damage, ~2–2.5-fold more unresolved DNA damage was estimated which remained in MSH6-deficient cells in comparison to control cells at 6 and 12 h after NCS or IR treatment (Figure 14A and B). These results demonstrate that MSH6 deficiency retards DNA repair of NCS-induced DNA-strand breaks.

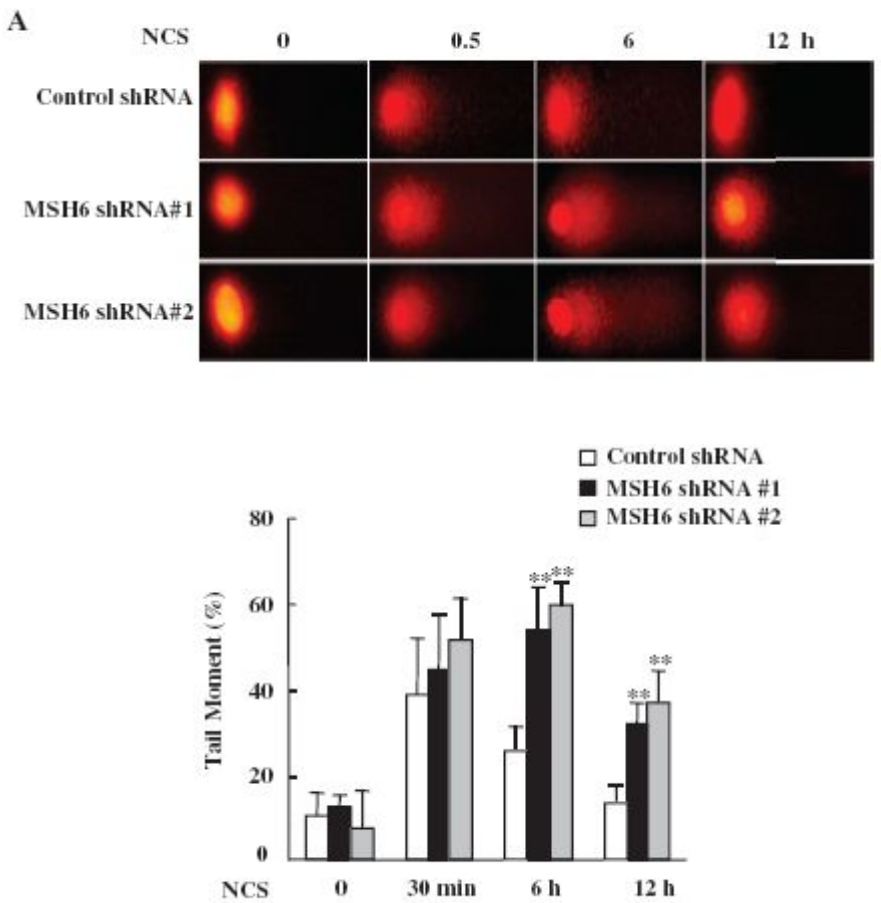

Figure 14 MSH6 knockdown results in decreased DSB repair

(A) Control and MSH6-depleted HeLa cells were untreated or treated with 100ng/ml NCS. At the indicated time points, cells were harvested for comet tail formation assays under alkaline conditions. Comet images were captured using fluorescence microscopy, and tail moment was analyzed in 75–80 randomly chosen comets using Komet 5.5 analysis software. Representative comet images observed at different time points after NCS treatment are shown. Changes show the percentage of relative comet tail moments between control and MSH6 knockdown

cells after treatment of NCS. Histograms represent the average of three independent experiments. Error bars represent the mean±SD. Asterisk denotes P<0.01.

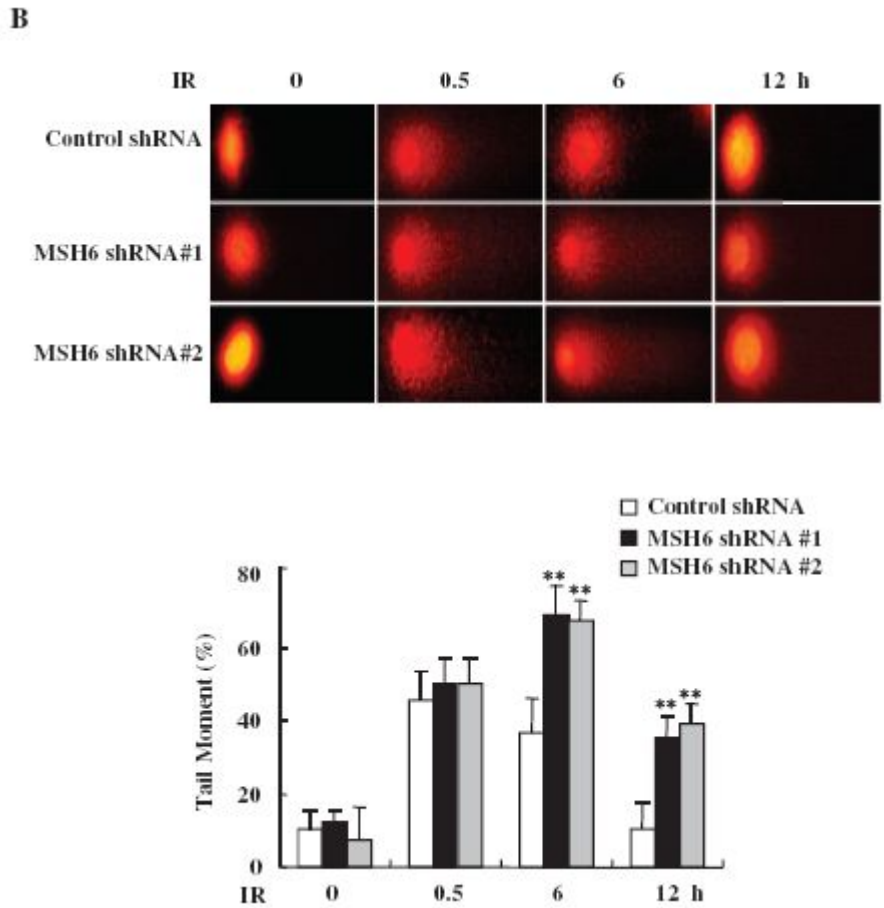

Figure 14 MSH6 knockdown sensitizes cells to DNA damage agents and DSB repair defect (B) Control and MSH6-depleted HeLa cells were untreated or treated with 5Gy ionizing radiation. At the indicated time points, cells were harvested for comet tail formation assays under alkaline conditions. Comet images were captured using fluorescence microscopy, and tail moment was analyzed in 75–80 randomly

chosen comets using Komet 5.5 analysis software. Representative comet images observed at different time points after NCS treatment are shown. Changes show the percentage of relative comet tail moments between control and MSH6 knockdown cells after treatment of ionizing radiation. Histograms represent the average of three independent experiments. Error bars represent the mean ±SD. Asterisk denotes $P<0.01$.

J. Sensitivity of MSH6 knockdown cell lines

Since radio-sensitivity of cells is also affected by proteins involved in DSB repair, the survival of cells depleted of MSH6 after exposure to NCS or IR was monitored. The sensitivity of the cells to NCS or IR was examined by assaying colony formation after NCS or IR treatment. The result showed that inhibition of MSH6 expression reduced the number of colonies formed within 15 days after treatment with 50 and 100 ng/ml NCS (Figure 15A) or 2 and 5 Gy IR (Figure 15B). Taken together, results from the functional analyses provide clear evidence that MSH6 is involved in the efficient repair of DSBs and is required for optimal cell survival following NCS- or IR-induced DNA damage.

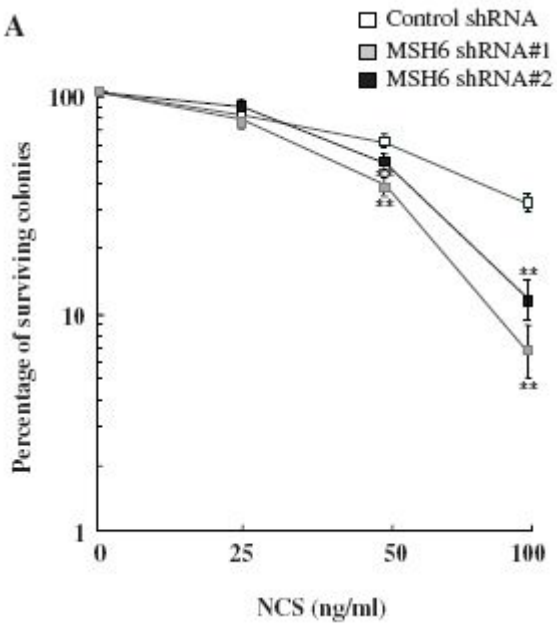

Figure 15 Sensitivity of the MSH6 depleted HeLa cells following exposure to NCS (A) Control and MSH6-knockdown HeLa cells were untreated or treated with the indicated doses of NCS and cell survival was assessed using a clonogenic assay. Data represent the mean±SD of three independent experiments. Asterisk denotes $P<0.01$.

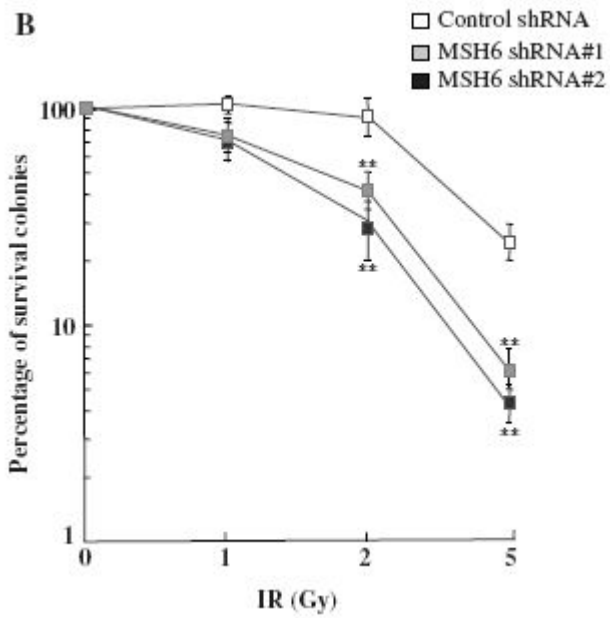

Figure 15 MSH6 depletion affects survival of HeLa cells following exposure to γ-irradiation. (B) Control and MSH6-knockdown HeLa cells were untreated or treated with the indicated doses of ionizing radiation and cell survival was assessed using a clonogenic assay. Data represent the mean±SD of three independent experiments. Asterisk denotes $P<0.01$.

IV. Discussion

MMR removes DNA mismatches that have evaded proofreading during DNA replication. This versatile postreplicative repair system efficiently corrects single-base mismatches and loops of up to 16 extrahelical nucleotides that arise during replication of repetitive DNA tracts (Harfe and Jinks-Robertson, 2000; Jiricny, 2006). Repair is initiated by binding of one of two mismatch recognition complexes that have overlapping specificities, ensuring efficient repair of all common replication errors. The MutSα and MutSβ mismatch recognition complexes are heterodimers of hMSH2/hMSH6 and hMSH2/hMSH3, respectively. The MutSα complex binds to and participates in the repair of single base–base mismatches and insertion/deletion loops, whereas the MutSβ complex recognizes insertion/deletion loops larger than the single-base mispairs (Gradia et al., 1997, Genschel et al., 1998). Another heterodimeric complex made up of hMLH1 and hPMS2 forms a ternary complex with the MutS complexes and promotes repair via its endonucleolytic activity, leading to excision repair of the mismatch (Kadyrov et al., 2006). In addition to their functions in post-replicative MMR, MMR proteins also participate in many cellular processes through associations with DNA-damage-signaling proteins. For example, MMR proteins, including MSH2, MSH6 and MLH1, are components of the BRCA- 1-associated genome surveillance complex, a multi-protein complex involved in the recognition and response to abnormal DNA structures (Wang et al., 2000). In addition, MSH2 constitutively interacts with the ATR kinase to form a signaling module that regulates phosphorylation of downstream effectors, such as Chk1 (Wang and Qin, 2003). MLH1 and MSH2 also act as adaptors that link ATM and Chk2 in response to DNA damage through associations with these proteins (Brown et al., 2003). PMS2 collaborates with p73

to enhance cisplatin-induced apoptosis (Shimodaira et al., 2003). The interaction between MMR and base excision repair pathways is critical for modulating the DNA-damage response (Kovtun and McMurray, 2007). The three MutL homologs, MLH1, PMS2 and PMS1, have been shown to interact with a large number of proteins involved in cell-cycle regulation, signaling and apoptosis (Cannavo et al., 2007). Therefore, identification of MMR-binding proteins and the functional significance of their interactions are important for understanding the myriad biological functions of these proteins.

In this study, mismatch repair protein MSH6 was shown to bind with Ku70 after DNA damage in endogenous and exogenous level. These finding suggest that DNA repair performed through NHEJ system is frequently impaired in MSH6 deficient cell and this might result in additional sensitivity in MSH6 deficient cell to Neocarzinostatin. Furthermore, MSH6 colocalized with Ku70 and γ -H2AX at the site of DNA damage and forms distinct foci after cell encounter DSBs.

A. MSH6 plays a potential role through binding with Ku70 and recruits at the site of double strand break

In this investigation, several independent observations are studied to document a specific interaction between mismatch repair protein MSH6 and Ku70. A Yeast two-hybrid assay is used to show that MSH6 interacts with Ku70. Furthermore, Ku70 co-immunoprecipitates with MSH6 from HeLa cell extracts and that this interaction is enhanced after radiomimetic NCS or IR exposure. MSH6 forms NCS- or IR-induced nuclear foci that colocalize with γ-H2AX at the sites of DNA breaks.

Recently, several lines of evidence suggest that MMR plays a role in repair of DSBs, which can be repaired by HR or NHEJ. However, the underlying

mechanisms by which MMR regulates DSB repair remain unknown. The present study shows that MSH6 is readily accumulated at the sites of DSBs, where it colocalizes with γ-H2AX after NCS or IR treatment. Previous reports show that MSH2 and MSH3 accumulate at the DNA double strand break side and colocalize with γ-H2AX (Hong et al., 2008). Co-immunoprecipitation experiments also reveals that MSH6 associates with Ku70 within 3 h after NCS treatment and that this interaction returns to basal levels at 12 h post-NCS treatment. In addition, endogenous MSH6 and Ku86 could be coimmunoprecipitated, and this is increased after treatment of NCS. On the other hand, endogenous MSH6 and endogenous DNA-PKcs did not interact in the absence of NCS, but upon NCS treatment the interaction was found. However, interaction between MSH6 and XRCC4 in the presence of NCS was not detected by coimmunoprecipitation. Together, these data suggest that MSH6 may relocalize to the DSB site following NCS or IR treatment and work together with Ku70 and play a role in early process of NHEJ in response to DNA damage. The N-terminus region of MSH6 plays the crucial role in respond to DNA damage (Hong et al., 2008). MSH6 has a PCNA binding motif, a large region of unknown function and a non specific DNA binding fragment in its N-terminus region (NTR). Furthermore, Laguri et al., 2008 has reported about human MSH6 NTR containing a globular PWWP domain in the region of unknown function binds to double stranded DNA. Indeed, involvement of PCNA in NHEJ of DSBs has been shown by the fact that depletion of cell extracts for PCNA resulted in a reduction in end-joining activity (Pospiech et al., 2001). So hereby, it can be anticipated that PCNA could be a factor which may influence the binding of MSH6 with Ku70 after NHEJ occur in the cell in response to NCS or IR. Overall, above all the possible reasons of MSH6 binding with Ku70 can not be excluded. Till date the N-terminus region of MSH6 has been shown to be important for DSBs response.

It has been suggested that the accumulation pattern of full length MSH6 in the DSBs site is slow (Hong et al., 2008). Exogenous immunoprecipitation assay shows that the binding was visible as early as 1hr post treatment. Notably, the band intensity of treated sample was significantly increased in compare to control. The binding in control cell could be a reason of post replication modification. Secondly, this result could predict the possibility of the presence of some other unknown region of human MSH6 gene through which MSH6 possibly response in error prone pathway by associating with Ku70, is yet to be discovered. It is been already suggested that DNA repair pathways are not separated but well interlinked (Zang et al., 2009). Thus, these data suggest that on the onset of NHEJ, MMR machinery could respond in cellular level and repair synthesis via Ku70 through a protein-protein interaction. This finding revealed previously unrecognized roles of MSH6 protein and indicates that a successful NHEJ repair requires both NHEJ repair mechanisms and MMR repair system. In conclusion, this study provides evidence for a direct role of MMR components (MSH6) in the NHEJ- mediated repair of DSB.

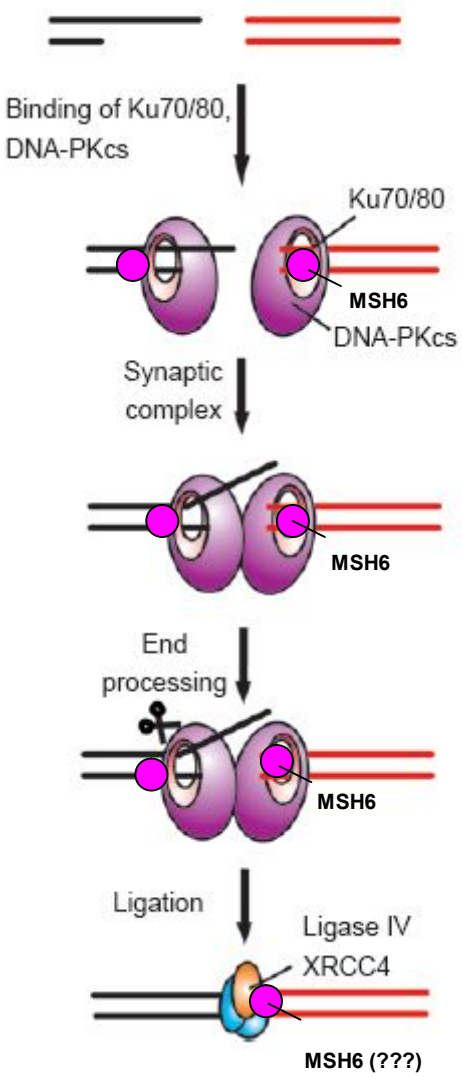

Figure16 A model for the involvement of Ku70/MSH6 in the regulation of NHEJ activity during the DSB damage response (Weterings and Chen, 2008)

B. Knockdown of MSH6 down-regulates NHEJ and sensitize/delay DNA DSB repair

DNA double Strand breaks (DSBs) are critical lesions that can result in cell death and lead to potentially oncogenis genomic rearrangements. Among the two DSBs repair pathway, NHEJ is the major and preferential repair pathway in human cells (Mao et al., 2008). NHEJ was previously reported to be decreased in MMR-deficient colon cancer cell lines in comparison to MMR-proficient cells (Koh et al., 2005). Since inactivating mutations frequently occur in the hRAD50 and hMRE11 genes in MMR-deficient tumors (Kim et al., 2001; Giannini et al., 2002), impaired expression of these proteins has been suggested to lead to decreased MRE11/RAD50/NBS1 complex formation, decreased NHEJ and increased sensitivity to IR. However, the MMR-deficient colon cancer cell line DLD1, which contains a mutation in the MSH6 gene (Papadopoulos et al., 1995), has normal hRAD50 and hMRE11 expression but still exhibits decreased NHEJ activity in comparison to MSH6- proficient cells (Koh et al., 2005). As described above, MSH6 was demonstrated to interact with Ku70 and that HeLa cells stably expressing MSH6 shRNAs exhibit impaired ability to repair DSBs. Thus, it seems reasonable to expect that MSH6 contributes directly to NHEJ activity. Using an in vivo repair assay that makes use of plasmids linearized with HindIII to generate non-complementary ends, direct evidence of MSH6 promoting DSB induced NHEJ was provided. MSH6-deficient HeLa cells were shown to exhibit a ~30% reduction in HindIII-induced NHEJ. To further confirm the effects of MSH6 on HindIII-induced NHEJ, DLD1 cells were rescued with MSH6. It was found that the overexpression of MSH6 in DLD1 cells increases NHEJ activity.

What possible roles do the MSH6 proteins play at the site of the NHEJ? The NHEJ process is initiated by the binding of a protein complex, the Ku70/80 heterodimer, to both ends of the broken DNA molecule which creates a scaffold for the assembly of the other NHEJ key enzymes (Weterings and Chen, 2008). The DNA-Ku- MSH6 scaffold can attracts the DNA-dependent protein kinase catalytic subunit (DNA-PKcs) to the DSB which brings both DNA ends together. Once the two DNA ends have been captured and tethered in a protein complex consisting of Ku and DNA-PKcs, non-ligatable DNA termini must be processed before final repair of the DSB can take place. Several enzymes have been identified at this point that are able to either remove or fill-in single-stranded, non-compatible overhangs. It is this step in the NHEJ process that is considered to be responsible for the deletion or insertion of one or several nucleotides prior to DSB healing, associated with NHEJ-mediated repair. In considering the known function of MSH6, one fact can be envision that at least two exclusive mechanisms by which MSH6 may be involved in NHEJ event. In this step, MMR machinery may respond to mis-paired bases produced as DNA termini interact. As a central protein of MMR system, MSH6 may respond and can bind directly with Ku70. Further, the bound MSH6 could recognize mispair bases and if encounter any mismatch bases that can be readily repaired by the MMR protein before processing to the final repair of NHEJ. As hMSH6 modify substrate specificity, these mismatch bases may be substrate for the DNA mismatch repair protein MSH6. In this scenario, all proteins critical to spell-checking would be expected to influence NHEJ. We note that it has been reported earlier, MSH2 and MSH3 localize to DSB site (Evans et al., 2000). It is reasonable to think that this affinity of MSH proteins for DNA ends may facilitate the assembly of complete and functional MMR machinery, including MSH6, at the

sites of end joining. Collectively, these results suggest that presence in MSH6 have a major impact on the overall efficiency of the error-prone NHEJ.

In second scenario, MSH6 may influence the NHEJ repair through binding with Ku70 and could further facilitate the association of other important NHEJ proteins to binds to the broken DNA ends. In the absence of MSH6 this overall influence of MMR protein will be dramatically decreased in NHEJ process which in turn can lower the NHEJ activity in the cell and can make the NHEJ process more dangerous if any mis-paired bases left behind. It is been already reported that mismatch repair protein MSH2, Mlh1 has a active participation in NHEJ. It is therefore, tempting to suppose that the biochemical and morphological observations, as well as functional analyses, provide compelling evidence for a nuclear complex consisting of MSH6 and Ku70.

C. Effect of MSH6 deficiency on cell survival and MMR activity on double strand DNA damage

MMR proteins participate in a number of cellular processes and function as a damage sensor. In this work, MSH6- deficient human HeLa cells were used to investigate whether MSH6 knockdown affected DSB repair using two different assays that measure the levels of DSBs in cells exposed to survival curve range doses of NCS or IR, the γ-H2AX and comet assays.

Comet assay was performed in the presence and absence of MSH6, showed comparable difference in tail length. The damage in the MSH6 deficient cell was high as compared to MSH6 proficient cell. To again recheck the same, clonogenic cell survival assay was performed which showed high sensitivity to DSB. In this work NCS and IR was used which induces sequence specific double strand breaks

in DNA. Clonogenic cell survival assay and comet assay revealed that MSH6 deficiency was related to cell death in response to NCS and IR and possessed high DNA damage.

Cell lines defective for any of the DSB repair genes are generally highly sensitive to IR and have marked deficiencies in DSB repair (Chang et al., 1993). Knockout or knockdown of Ku70 (Omori et al., 2002, Ayene et al., 2005) or DNA-PKcs (Peng et al., 2002) has been shown to result in hypersensitivity to radiation. Loss of MMR activity generally renders cells less sensitive to cell killing by DNA-damaging agents, reflecting the role(s) of the MMR system in DNA-damage signaling used to trigger cell-cycle arrest and apoptosis (Meyers et al., 2004, Stojic et al., 2004).A similar high sensitivity to the DNA DSB producing drug, Bleomycin had also been reported for MMR- deficient cell lines (Li et al., 2004). It has been also suggested that MMR deficiency lead to higher sensitivity to γ-irradiation in MMR deficient cell lines (Koh et al., 2005).

Next γ-H2AX phosphorylation and colocalization after DNA damage in response to NCS and IR was performed in HeLa cell lines. These data supported the fact that MSH6 knockdown cell showed up distinct γ-H2AX foci in all MSH6 deficient cell till 6hr post treatments whereas in the control cell, γ-H2AX foci was significantly less indicating the fact that most of the DNA DSBs were repaired by then . This result suggests that MSH6 deficient cells were more prone to DSB formation and were unable to repair the DSBs in the absence of intact MMR machinery. Furthermore, to verify whether MSH6 forms foci at the DSBs site, MSH6 foci were investigated using immunofluorescence microscopy.

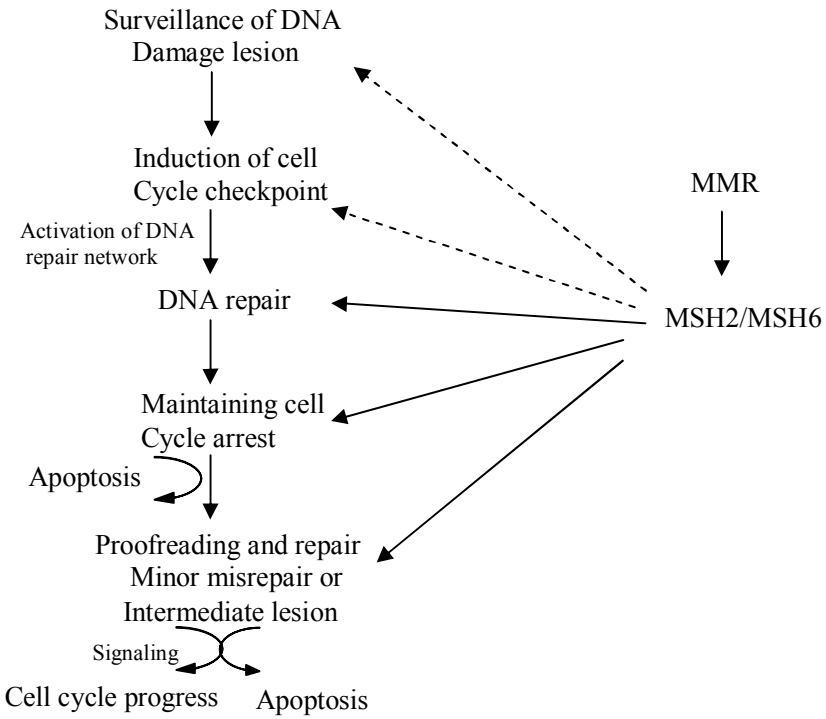

Figure 17 The proposed linkage interlink between MMR and DSB process (Zhang et al., 2009)

Interestingly, MSH6 was readily visible at the site of DSBs post 1hr of treatment and were localized with γ-H2AX. All over, these data supported the fact that formation of DSB can sensitize MSH6 protein to recruit at the site of DSBs. Over recruitment, MSH6 can facilitate systematic repair machinery and binds to Ku70. MSH6 binds to NHEJ complex till the NHEJ process reaches the final step and can recognize any mismatch that arises during NHEJ process. After correcting the mismatches, MSH6 dissociates from the site of the DSBs and the final ligation

reaction may be enhanced by the presence of the recently discovered XLF/Cernunnos protein. In endogenous immunoprecipitation assay, a decreased pattern of MSH6 and Ku70 binding over time has been reported and comes to basal level as untreated condition. This result also matched with the colocalization assay performed to check the association of MSH6 and Ku70. Thus, altogether these data shows a direct role of MSH6 in double strand break repair via NHEJ through a binding with Ku70. Till date, many MMR proteins have been implicated in DSB repair. MSH2, MSH3 and MLH1 have been already shown to participate in NHEJ pathway (Smith et al., 2005, Bannister et al., 2004).

Nonetheless, NHEJ is a complex repair process and refer to error- prone pathway. Induction of NHEJ process not only signalizes the well known NHEJ protein but can also activate the other non-NHEJ repair pathway which further activates the particular protein necessary for the repair. MSH6 is a highly conserved and central repair protein that may physically facilitates NHEJ machinery has to be determined. The X-ray crystal structure of Ku shows that it binds to DNA via a channel generated by heterodimer formation (Walker et al., 2001). Thus, the MSH6 could further increase the binding affinity of Ku for DNA, modulate the amount of Ku70/80 heterodimer complexes or facilitate the recruitment of other important NHEJ proteins to bind the broken-DNA ends. The ability of recognizing mismatch bases may allow MSH6 to participate in damage surveillance. Further study is necessary for a more detailed understanding of MSH6 mechanism in DNA double strand break repair.

References

Amsel, A.D., Rathaus, M., Kronman, N., and Cohen, H.Y. (2008). Regulation of the proapoptotic factor Bax by Ku70-dependent deubiquitylation. Proc Natl Acad Sci U S A *105*, 5117-5122.

Ayene, I.S., Ford, L.P., and Koch, C.J. (2005). Ku protein targeting by Ku70 small interfering RNA enhances human cancer cell response to topoisomerase II inhibitor and gamma radiation. Mol Cancer Ther *4*, 529-536.

Bannister, L.A., Waldman, B.C., and Waldman, A.S. (2004). Modulation of error-prone double-strand break repair in mammalian chromosomes by DNA mismatch repair protein Mlh1. DNA Repair (Amst) *3*, 465-474.

Brown, K.D., Rathi, A., Kamath, R., Beardsley, D.I., Zhan, Q., Mannino, J.L., and Baskaran, R. (2003). The mismatch repair system is required for S-phase checkpoint activation. Nat Genet *33*, 80-84.

Cannavo, E., Gerrits, B., Marra, G., Schlapbach, R., and Jiricny, J. (2007). Characterization of the interactome of the human MutL homologues MLH1, PMS1, and PMS2. J Biol Chem *282*, 2976-2986.

Chai, W., Ford, L.P., Lenertz, L., Wright, W.E., and Shay, J.W. (2002). Human Ku70/80 associates physically with telomerase through interaction with hTERT. J Biol Chem *277*, 47242-47247.

Chang, C., Biedermann, K.A., Mezzina, M., and Brown, J.M. (1993). Characterization of the DNA double strand break repair defect in scid mice. Cancer Res *53*, 1244-1248.

Cohen, H.Y., Lavu, S., Bitterman, K.J., Hekking, B., Imahiyerobo, T.A., Miller, C., Frye, R., Ploegh, H., Kessler, B.M., and Sinclair, D.A. (2004). Acetylation of the C terminus of Ku70 by CBP and PCAF controls Bax-mediated apoptosis. Mol Cell *13*, 627-638.

Collis, S.J., DeWeese, T.L., Jeggo, P.A., and Parker, A.R. (2005). The life and death of DNA-PK. Oncogene *24*, 949-961.

Elliott, B., and Jasin, M. (2001). Repair of double-strand breaks by homologous recombination in mismatch repair-defective mammalian cells. Mol Cell Biol *21*, 2671-2682.

Evans, E., Sugawara, N., Haber, J.E., and Alani, E. (2000). The Saccharomyces cerevisiae Msh2 mismatch repair protein localizes to recombination intermediates in vivo. Mol Cell *5*, 789-799.

Fang, L., Wang, Y., Du, D., Yang, G., Tak Kwok, T., Kai Kong, S., Chen, B., Chen, D.J., and Chen, Z. (2007). Cell polarity protein Par3 complexes with DNA-PK via Ku70 and regulates DNA double-strand break repair. Cell Res *17*, 100-116.

Genschel, J., Littman, S.J., Drummond, J.T., and Modrich, P. (1998). Isolation of MutSbeta from human cells and comparison of the mismatch repair specificities of MutSbeta and MutSalpha. J Biol Chem *273*, 19895-19901.

Giannini, G., Ristori, E., Cerignoli, F., Rinaldi, C., Zani, M., Viel, A., Ottini, L., Crescenzi, M., Martinotti, S., Bignami, M*., et al.* (2002). Human MRE11 is inactivated in mismatch repair-deficient cancers. EMBO Rep *3*, 248-254.

Gradia, S., Acharya, S., and Fishel, R. (1997). The human mismatch recognition complex hMSH2-hMSH6 functions as a novel molecular switch. Cell *91*, 995-1005.

Grawunder, U., Zimmer, D., Fugmann, S., Schwarz, K., and Lieber, M.R. (1998). DNA ligase IV is essential for V(D)J recombination and DNA double-strand break repair in human precursor lymphocytes. Mol Cell *2*, 477-484.

Harfe, B.D., and Jinks-Robertson, S. (2000). DNA mismatch repair and genetic instability. Annu Rev Genet *34*, 359-399.

Hong, Z., Jiang, J., Hashiguchi, K., Hoshi, M., Lan, L., and Yasui, A. (2008). Recruitment of mismatch repair proteins to the site of DNA damage in human cells. J Cell Sci *121*, 3146-3154.

Hsieh, P., and Yamane, K. (2008). DNA mismatch repair: molecular mechanism, cancer, and ageing. Mech Ageing Dev *129*, 391-407.

Iyer, R.R., Pluciennik, A., Burdett, V., and Modrich, P.L. (2006). DNA mismatch repair: functions and mechanisms. Chem Rev *106*, 302-323.

Jacob, S., Miquel, C., Sarasin, A., and Praz, F. (2005). Effects of camptothecin on double-strand break repair by non-homologous end-joining in DNA mismatch repair-deficient human colorectal cancer cell lines. Nucleic Acids Res *33*, 106-113.

Jiricny, J. (2006). The multifaceted mismatch-repair system. Nat Rev Mol Cell Biol *7*, 335-346.

Kadyrov, F.A., Dzantiev, L., Constantin, N., and Modrich, P. (2006). Endonucleolytic function of MutLalpha in human mismatch repair. Cell *126*, 297-308.

Kang, Y., Lee, J.H., Hoan, N.N., Sohn, H.M., Chang, I.Y., and You, H.J. (2009). Protein phosphatase 5 regulates the function of 53BP1 after neocarzinostatin-induced DNA damage. J Biol Chem *284*, 9845-9853.

Karmakar, P., Snowden, C.M., Ramsden, D.A., and Bohr, V.A. (2002). Ku heterodimer binds to both ends of the Werner protein and functional interaction occurs at the Werner N-terminus. Nucleic Acids Res *30*, 3583-3591.

Karran, P. (2000). DNA double strand break repair in mammalian cells. Curr Opin Genet Dev *10*, 144-150.

Khanna, K.K., and Jackson, S.P. (2001). DNA double-strand breaks: signaling, repair and the cancer connection. Nat Genet *27*, 247-254.

Kim, N.G., Choi, Y.R., Baek, M.J., Kim, Y.H., Kang, H., Kim, N.K., Min, J.S., and Kim, H. (2001). Frameshift mutations at coding mononucleotide repeats of the hRAD50 gene in gastrointestinal carcinomas with microsatellite instability. Cancer Res *61*, 36-38.

Koh, K.H., Kang, H.J., Li, L.S., Kim, N.G., You, K.T., Yang, E., Kim, H., Kim, H.J., Yun, C.O., and Kim, K.S. (2005). Impaired nonhomologous end-joining in mismatch repair-deficient colon carcinomas. Lab Invest *85*, 1130-1138.

Koike, M., Shiomi, T., and Koike, A. (2001). Dimerization and nuclear localization of ku proteins. J Biol Chem *276*, 11167-11173.

Kovtun, I.V., and McMurray, C.T. (2007). Crosstalk of DNA glycosylases with pathways other than base excision repair. DNA Repair (Amst) *6*, 517-529.

Laguri, C., Duband-Goulet, I., Friedrich, N., Axt, M., Belin, P., Callebaut, I., Gilquin, B., Zinn-Justin, S., and Couprie, J. (2008). Human mismatch repair protein MSH6 contains a PWWP domain that targets double stranded DNA. Biochemistry *47*, 6199-6207.

Li, B., and Comai, L. (2000). Functional interaction between Ku and the werner syndrome protein in DNA end processing. J Biol Chem *275*, 39800.

Li, G.M. (2008). Mechanisms and functions of DNA mismatch repair. Cell Res *18*, 85-98.

Li, H.R., Shagisultanova, E.I., Yamashita, K., Piao, Z., Perucho, M., and Malkhosyan, S.R. (2004). Hypersensitivity of tumor cell lines with microsatellite instability to DNA double strand break producing chemotherapeutic agent bleomycin. Cancer Res *64*, 4760-4767.

Li, Z., Otevrel, T., Gao, Y., Cheng, H.L., Seed, B., Stamato, T.D., Taccioli, G.E., and Alt, F.W. (1995). The XRCC4 gene encodes a novel protein involved in DNA double-strand break repair and V(D)J recombination. Cell *83*, 1079-1089.

Lieber, M.R., Ma, Y., Pannicke, U., and Schwarz, K. (2003). Mechanism and regulation of human non-homologous DNA end-joining. Nat Rev Mol Cell Biol *4*, 712-720.

Mao, Z., Bozzella, M., Seluanov, A., and Gorbunova, V. (2008). DNA repair by nonhomologous end joining and homologous recombination during cell cycle in human cells. Cell Cycle *7*, 2902-2906.
Mazumder, S., Plesca, D., Kinter, M., and Almasan, A. (2007). Interaction of a cyclin E fragment with Ku70 regulates Bax-mediated apoptosis. Mol Cell Biol *27*, 3511-3520.

Meyers, M., Hwang, A., Wagner, M.W., and Boothman, D.A. (2004). Role of DNA mismatch repair in apoptotic responses to therapeutic agents. Environ Mol Mutagen *44*, 249-264.

Mimori, T., Hardin, J.A., and Steitz, J.A. (1986). Characterization of the DNA-binding protein antigen Ku recognized by autoantibodies from patients with rheumatic disorders. J Biol Chem *261*, 2274-2278.

Nolens, G., Pignon, J.C., Koopmansch, B., Elmoualij, B., Zorzi, W., De Pauw, E., and Winkler, R. (2009). Ku proteins interact with activator protein-2 transcription factors and contribute to ERBB2 overexpression in breast cancer cell lines. Breast Cancer Res *11*, R83.

Omori, S., Takiguchi, Y., Suda, A., Sugimoto, T., Miyazawa, H., Tanabe, N., Tatsumi, K., Kimura, H., Pardington, P.E., Chen, F.*, et al.* (2002). Suppression of a DNA double-strand break repair gene, Ku70, increases radio- and chemosensitivity in a human lung carcinoma cell line. DNA Repair (Amst) *1*, 299-310.

Papadopoulos, N., Nicolaides, N.C., Liu, B., Parsons, R., Lengauer, C., Palombo, F., D'Arrigo, A., Markowitz, S., Willson, J.K., Kinzler, K.W.*, et al.* (1995). Mutations of GTBP in genetically unstable cells. Science *268*, 1915-1917.

Peng, Y., Zhang, Q., Nagasawa, H., Okayasu, R., Liber, H.L., and Bedford, J.S. (2002). Silencing expression of the catalytic subunit of DNA-dependent protein kinase by small interfering RNA sensitizes human cells for radiation-induced chromosome damage, cell killing, and mutation. Cancer Res *62*, 6400-6404.

Pospiech, H., Rytkonen, A.K., and Syvaoja, J.E. (2001). The role of DNA polymerase activity in human non-homologous end joining. Nucleic Acids Res *29*, 3277-3288.

Rogakou, E.P., Pilch, D.R., Orr, A.H., Ivanova, V.S., and Bonner, W.M. (1998). DNA double-stranded breaks induce histone H2AX phosphorylation on serine 139. J Biol Chem *273*, 5858-5868.

Shimodaira, H., Yoshioka-Yamashita, A., Kolodner, R.D., and Wang, J.Y. (2003). Interaction of mismatch repair protein PMS2 and the p53-related transcription factor p73 in apoptosis response to cisplatin. Proc Natl Acad Sci U S A *100*, 2420-2425.

Shrivastav, M., De Haro, L.P., and Nickoloff, J.A. (2008). Regulation of DNA double-strand break repair pathway choice. Cell Res *18*, 134-147.
Smith, J.A., Waldman, B.C., and Waldman, A.S. (2005). A role for DNA mismatch repair protein Msh2 in error-prone double-strand-break repair in mammalian chromosomes. Genetics *170*, 355-363.

Stewart, G.S., Wang, B., Bignell, C.R., Taylor, A.M., and Elledge, S.J. (2003). MDC1 is a mediator of the mammalian DNA damage checkpoint. Nature *421*, 961-966.

Stojic, L., Brun, R., and Jiricny, J. (2004). Mismatch repair and DNA damage signalling. DNA Repair (Amst) *3*, 1091-1101.

Sugawara, N., Paques, F., Colaiacovo, M., and Haber, J.E. (1997). Role of Saccharomyces cerevisiae Msh2 and Msh3 repair proteins in double-strand break-induced recombination. Proc Natl Acad Sci U S A *94*, 9214-9219.

Tanaka, Y., Imamura, J., Kanai, F., Ichimura, T., Isobe, T., Koike, M., Kudo, Y., Tateishi, K., Ikenoue, T., Ijichi, H.*, et al.* (2007). Runx3 interacts with DNA repair protein Ku70. Exp Cell Res *313*, 3251-3260.

Ting, N.S., Yu, Y., Pohorelic, B., Lees-Miller, S.P., and Beattie, T.L. (2005). Human Ku70/80 interacts directly with hTR, the RNA component of human telomerase. Nucleic Acids Res *33*, 2090-2098.

Tuteja, R., and Tuteja, N. (2000). Ku autoantigen: a multifunctional DNA-binding protein. Crit Rev Biochem Mol Biol *35*, 1-33.

Walker, J.R., Corpina, R.A., and Goldberg, J. (2001). Structure of the Ku heterodimer bound to DNA and its implications for double-strand break repair. Nature *412*, 607-614.

Wang, Y., Cortez, D., Yazdi, P., Neff, N., Elledge, S.J., and Qin, J. (2000). BASC, a super complex of BRCA1-associated proteins involved in the recognition and repair of aberrant DNA structures. Genes Dev *14*, 927-939.

Wang, Y., and Qin, J. (2003). MSH2 and ATR form a signaling module and regulate two branches of the damage response to DNA methylation. Proc Natl Acad Sci U S A *100*, 15387-15392.

Weterings, E., and Chen, D.J. (2008). The endless tale of non-homologous end-joining. Cell Res *18*, 114-124.

Yin, H., and Glass, J. (2006). In prostate cancer cells the interaction of C/EBPalpha with Ku70, Ku80, and poly(ADP-ribose) polymerase-1 increases sensitivity to DNA damage. J Biol Chem *281*, 11496-11505.

Zhang, Y., Rohde, L.H., and Wu, H. (2009). Involvement of nucleotide excision and mismatch repair mechanisms in double strand break repair. Curr Genomics *10*, 250-258.

ABSTACT

The role of MMR on the Non-Homologous End Joining Activity

Ankita Shahi (De)
Advisor: Prof. Ho Jin You, M.D., Ph.D.
Department of Bio-materials
Graduate School of Chosun University

MSH6, a key component of the MSH2–MSH6 complex, plays a fundamental role in the repair of mismatched DNA bases. Recent studies have presented increasing evidence that various DNA repair pathways are not separated, but well interlinked. It has been suggested that non-DSB repair mechanisms, Mismatch Repair (MMR) is highly involved in DSB repairs. These findings revealed previously unrecognized roles of various MMR proteins and indicated that a successful DSB repair requires both DSB repair mechanisms and non-DSB repair systems. In this report, MSH6 was found to be a novel Ku70-interacting protein identified by yeast two-hybrid screening. Ku70 and Ku86 are two key regulatory subunits of the DNA-dependent protein kinase, which plays an essential role in repair of DNA double-strand breaks (DSBs) through the non-homologous end-joining (NHEJ) pathway. Endogenous binding of MSH6 and Ku70 was enhanced in response to treatment with the radiomimetic drug neocarzinostatin (NCS) or

ionizing radiation (IR), a potent inducer of DSBs. A direct association between Ku70 and a full length MSH6 had also been reported in this work. Furthermore, MSH6 exhibited diffuse nuclear staining in the majority of untreated cells and formed discrete nuclear foci after NCS or IR treatment.

MSH6 co- localized with Ku70 at the site of DNA damage after NCS or IR treatment and was bind to γ-H2AX. Cells depleted of MSH6 accumulated high levels of persistent DSBs, as detected by formation of γ -H2AX foci and by the comet assay. Notably, NHEJ activity in the MSH6 suppressed cell was significantly decreased compared to the control cell and rescued after the restoration of MSH6 in the deficient cell line DLD1. MSH6 deficient cells were hypersensitive to NCS- or IR-induced cell death, as revealed by a clonogenic cell-survival assay. These result indicated the influence of MMR protein MSH6 in DSB repair through upregulation of NHEJ by association with Ku70. The combined results suggested that MSH6 plays a potential role in DSB repair. Although MMR proteins are known to influence cellular responses to DNA damage, how MMR proteins respond to DNA damage with in the cell remain unknown. Moreover, the data indicated MMR protein MSH6 not only has active participation in mismatch repair produced during replication but also recruited to the site of NHEJ repair in human cells and depletion of MSH6 decreases the efficiency of Non homologous end joining.

ACKNOWLEDGEMENT

It is a pleasure to thank the many people who made this thesis possible.

First and foremost, I would like to express my sincere gratitude to my academic advisor Prof. Ho Jin You for the continuous heart whelming full support of my Ph.D. study and research, for his patience, motivation, enthusiasm, immense knowledge and his great efforts to explain things clearly and simply. His guidance helped me in all the time of research and throughout my thesis-writing period, he provided encouragement, sound advice, good teaching, good company, and lots of good ideas. I could not have imagined having a better advisor and mentor for my Ph.D. study.

I would like to thank Prof. In-Youb Chang for his kind assistance and helping me medically to get through the difficult times, and for all the emotional support, and caring he provided.

Besides my advisor, I would like to thank the rest of my thesis committee: Prof. Jung-Hee Lee, Prof. Jae-Yeoul Jun, and Prof. Young- Jin Jeon.

It is difficult to overstate my sincere thanks to Prof. Jung-Hee Lee who has taught me, both consciously and un-consciously, how good experimental biology is done. I appreciate all her contributions of time, ideas to make my Ph.D. experience productive and stimulating. The joy and enthusiasm she has for her research was contagious and motivational
for me, even during tough times in the Ph.D. pursuit. I am also thankful for the excellent example she has provided as a successful woman biologist and professor.

I would also like to acknowledge my special thanks to Dr. Cha- Kyung Youn, Dr. Yoonsung Kang, Dr. P.N. Amatya and Dr. Seon- Joo Park who deserve special mention for their support during my course work. I have appreciated their collaboration and the impressive skills.

I thank my fellow past and present group members of the KDRRC group who have contributed immensely to my personal and professional time at Chosun. The group has been a source of friendships as well as good advice and collaboration. I am indebted to my many KDRRC colleagues for providing a stimulating and fun environment in which to learn and grow. I am especially grateful to Minji Kim and Na-Hee Kim, who were always ready to help me get through the difficult times, and for all the emotional support, camaraderie, entertainment, and caring they both provided.

Last but not the least; I would like to thank my entire extended family for all their love and encouragement. I sincerely thank my parents who raised me with a love of science and supported me in all my pursuits. My brother and In-laws were particularly supportive. And most of all for my loving, supportive, encouraging, and patient husband whose faithful support during this Ph.D. is so appreciated. Thank you.

Ankita Shahi (De)
Chosun University